EMBRITTLEMENT OF CU-17Al ALLOY BY LIQUID MERCURY

EMBRITTLEMENT OF CU-17Al ALLOY BY LIQUID MERCURY

By

PETER COLIN HANCOCK, B.Sc.

A Thesis

Submitted to the Faculty of Graduate Studies

in Partial Fulfilment of the Requirements

for the Degree

Master of Science

McMaster University

July 1967

ACKNOWLEDGEMENTS

The author wishes to acknowledge the invaluable advice and encouragement of Professor M. B. Ives and Professor J. D. Embury.

The work was supported by the U. S. Office of Naval Research and the author also acknowledges the receipt of a Shell Canada Limited Research Scholarship.

ABSTRACT

The role of plastic deformation in the initiation and propagation of cracks in Cu-17Al alloy embrittled by liquid mercury has been studied. It is proposed that extensive plastic deformation and work hardening must occur at the crack-tip during propagation in order to raise the local flow stress to a critical level at which the maximum normal stress is equal to the cohesive strength. A crack initiation mechanism is proposed involving grain boundary diffusion enhanced by the stress concentration at the head of dislocation pile-ups at the grain boundary. Micro-cracks are formed at the weakened grain boundary and a period of stable crack growth made over a period of increasing applied stress may be necessary before the crack is long enough to become unstable.

TABLE OF CONTENTS

LIST OF FIGURES

LIST OF PLATES

LIST OF TABLES

CHAPTER 4

APPENDIX

CHAPTER 1

Introduction

When copper-aluminum solid solutions are deformed in a mercury environment, intergranular fracture occurs at strains which are usually low but well beyond the yield point elongation. For example, in uniaxial tensile tests with a liquid mercury environment, Pargeter and Ives (1967.a) observed fracture strains in pure copper and Cu-17 at.%Al polycrystals of 0.20 and 0.03 respectively. The onset of failure is sudden with no prior changes in the stress-strain curve. Crack propagation velocities are very fast relative to stress-corrosion cracking, but much less than the velocities observed for brittle cracks in steel.

Due in great part to the multiplicity of slip systems and to the lack of sensitivity of flow stress to changes in strain rate and temperature, face-centred cubic metals and alloys do not undergo brittle cleavage fracture unless exposed to corrosive media or unless segregation to grain boundaries of an embrittling solute occurs. Copper-aluminum solid solutions are however extremely ductile and show no signs of grain boundary weakness when deformed in inert environments. The binary systems Cu/Hg and Al/Hg have very low solubilities of less than 0.005% and no evidence of penetration by the mercury has been observed except under stress and only very close to fracture. Pure polycrystalline copper has also been shown to be susceptible to mercury embrittlement by Pargeter and Ives (1967); pure metals are not susceptible to stress corrosion cracking. The embrittlement of copper and Cu-Al solid solution alloys by mercury therefore exhibits

basic differences from corrosion and stress-corrosion and fits into the class of phenomena referred to as 'liquid-metal embrittlement'.

Attempts to explain liquid-metal embrittlement have usually been based on the Griffith (1921) approach which essentially applies the First Law of Thermodynamics to the fracture process. Griffith's criterion for crack propagation states that the loss of elastic energy stored in the stressed system caused by the extension of a crack must be equal to or greater than the work required to create the two fracture surfaces before crack propagation can occur. This is a necessary but not always sufficient condition for any fracture process. The original work by Griffith was done on brittle fracture in glass and the work to create the fracture surfaces was equated to the true surface energy γ_s for a crack of length c and crack tip radius of atomic dimensions, the stress for propagation was given by a formula of the type:

$$\sigma = \left(\frac{E\gamma_s}{c} \right)^{1/2}$$

where E is Young's modulus.

The surface energy of copper in many liquid metal environments is known to be drastically reduced, sometimes by a factor of 5 or more below the value for copper in air. Before this criterion can be made adequate however, the crack initiation mechanism must be explained and any other crack tip processes and contributions to the work of fracture must be considered. Orowan (1949), in applying the Griffith approach to brittle fracture in metals proposed that a term p should be added to the surface energy γ_s to account for any plastic deformation occurring at the crack tip. During subsequent experiments Orowan estimated from X-ray Laue patterns that p was of the order 10^6 ergs/cm^2. for brittle fracture

of steel plate specimens at room temperature. Since this value is three orders of magnitude greater than γ_s Orowan considered that the value of the p controlled the fracture process and that γ_s, being small, could be neglected. In applying Orowan's modified formula to liquid-metal embrittlement it is immediately obvious that unless p and γ_s are interdependent then p can be no greater than the order of magnitude of γ_s if the Griffith criterion alone is to be a sufficient condition for the propagation of a crack. Gilman (1959) has put forward an argument to establish such an interdependence. Fracture is assumed to occur when the normal stress at the crack tip reaches the value of the cohesive strength. The cohesive strength itself is shown to be a function of the true surface energy. Gilman then argues that since fracture is observed to have occurred the maximum normal stress must have attained the value of the cohesive strength. Since the latter is controlled by the true surface energy then so is the former; and since there is a relationship between the shear stress distribution and the normal stress distribution, the surface energy will also determine the maximum shear stress. If, in an element δV in the vicinity of the crack, the maximum shear stress reached is τ then Gilman's analysis gives the energy of deformation $\delta(\gamma_p)$ as:

$$\delta(\gamma_p) = \frac{\tau^2}{2g} \delta V$$

where g is the shear modulas. The value of the true surface energy γ_s therefore controls the value of γ_p, the work per unit volume associated with plastic deformation during fracture, and γ_p decreases as γ_s decreases. If the assumptions are accepted then this argument provides a useful thermodynamic criterion for liquid-metal embrittlement.

The present state of the physical theory of cohesion in solids

makes it unreasonable to expect in the near future a complete theory which can predict fracture behaviour without resort to some kind of criterion such as that of a critical normal stress. At present the postulation of some criterion is necessary if fracture theory is to make any advance. Where such criteria are needed however it is essential to make a good assessment of their physical justification, and to this end it is essential in developing a fracture theory to obtain a physical description of all processes occurring at the crack tip. The Griffith-Orowan theory incorporating Gilman's argument for the role of true surface energy, may provide a useful method for obtaining such a description in the case of zinc embrittled by mercury, since zinc can also be made to cleave in a brittle manner in an inert environment making comparative experiments possible. (See for instance, Westwood, (1962), (1965)). In the case of face-centred cubic metals and alloys no such comparison is possible since in the absence of an embrittling environment these metals will fail only by ductile rupture. On Gilman's model it must be concluded that in an inert environment the cohesive strength is never attained. This also applies in the case where the metal, under stress, contains a crack of the same tip geometry as that which would propagate if an embrittling liquid metal was present. Proof of this is given by an experiment on a Cu-17 Al solid solution polycrystal deformed in uniaxial tension with a mercury coating on the gauge length. The quantity of mercury applied was sufficient to initiate a crack but insufficient to cause propagation through the entire cross section. When the mercury supply became insufficient to maintain embrittled conditions the crack ceased to propagate. The specimen deformed as it would in air when containing a sharp notch and eventually failed in

ductile rupture. The difference in the behaviour of Cu-17 Al between deformation in air and deformation in mercury is not therefore due only to the differences in stress systems associated with the presence or absence of cracks or with different shapes of crack tips. The inability of this alloy to sustain a brittle crack in the absence of mercury can only be ascribed to the effect of shear processes which in spite of a continuously increasing applied stress, prevents the normal stress at the crack tip from reaching the value of the cohesive strength. The effect of shear processes will be to reduce the elastic strain energy, which implies a reduction in the local stress concentrations at the crack tip, presumably by a 'blunting' of the crack tip profile. The extent of stress relaxation will be limited by strain hardening as long as the strain hardening rate is positive, (i.e. as long as ductile rupture processes do not intervene). Any factors which influence the strain hardening rate such as proximity of grain boundaries to the crack tip or ease of cross slip will also affect the capacity for relaxation of stress concentrations. The crystal system will be important in this respect and a close-packed hexagonal metal such as zinc with only three available slip systems at room temperature will have a much more limited capacity for stress relaxation than face-centred cubic metals with their multiplicity of possible slip systems. Stress relaxation by plastic deformation at the crack tip will also be limited by elastic constraints and hydrostatic stresses which may exist, especially for a specimen not in a state of general yield. These same tendencies for shear processes to reduce the local stress concentrations will also operate in metals deformed in an embrittling liquid metal environment wherever the shear stresses exceed the local flow stress.

Account must be taken where necessary however for effects of crack velocity with respect to strain rate sensitivity of the flow stress, dislocation mobility and delayed yield effects. Copper and copper solid-solution alloys, when deformed in embrittling liquid-metal environments, always extend well beyond general yield before fracturing. Since crack velocities are observed to be slow and the strain rate sensitivity of the flow stress is small, it seems quite possible therefore that extensive deformation may accompany fracture.

Gilman (1959) was aware of the considerable effect that shear processes might have on the stress distribution but did not develop the consequences of such effects in his fracture model beyond the statement that the derived value of γ_p would be an underestimate though still determined by γ_s. Because Gilman used an a posteriori argument, taking the fracture and accompanying deformation as observed facts to be explained rather than possible effects to be predicted, he presumably concluded that the normal stress at the crack tip was raised to the value of the cohesive strength despite the competitive action of the shear processes. The limiting effect of strain hardening on the stress relaxation processes may well provide a possible mechanism for this and it is discussed later.

An adequate fracture criterion has not yet been devised in terms of measurable stress and strain parameters, and the role of shear processes during crack propagation is only partly understood. In the case of metals embrittled by any sort of surface active environment there is an additional complicating factor in the interactions occurring at the crack tip. In approaching any fracture problem therefore, and particularly a complex one such as liquid-metal embrittlement, it is preferable to make as few

prior assumptions about fracture criteria as possible. It is unlikely that much progress can be made without assuming some kind of crack-tip model but it would seem more informative and certainly a better test of the adequacy of present knowledge and experimental data to regard crack-tip processes such as loss of cohesion and plastic deformation as possible occurrences to be predicted, rather than established facts to be explained. One approach of the former kind is to imagine a small sensor situated in the path of a crack and to attempt to predict the effects which the sensor would record if either the applied stress across a stationary crack was continuously increased or if the crack with its accompanying stress field moved towards the sensor. Kelly et al. (1967) have approached fracture theory in a similar way with the purpose of determining the abilities of a variety of dislocation-free solids to support a truly brittle crack. In the next section the theory is discussed and an attempt has been made to apply Kelly's approach to the fracture of copper and Cu-17 Al alloy deformed in a mercury environment. At the point of fracture these metals are far from being dislocation free however and some modifications to the theory are necessary in order to comply with physical realities. These modifications inevitably weaken the theory but the method of approach is still very informative.

The considerations which have been discussed above apply to the continued propagation of an existing crack and give no indication of how cracks can form. It has usually been assumed in the past that the critical process in liquid-metal embrittlement is the initiation rather than the propagation of a crack; the initiation stage, however, is very difficult to study experimentally. It has been at least partially substantiated

that in the brittle fracture of body-centred cubic and close packed hexagonal metals, brittle cracks are formed as a result of shear processes: micro-cracks may be formed on yielding or ductile ruptures at strain concentrations may be transformed into brittle cracks through the strain rate sensitivity of the flow stress. Normally, however, face-centred cubic metals are not susceptible to these modes of fracture. It has been observed by Westwood (1965) that some degree of plastic deformation seems to be a prerequisite for crack initiation in an embrittling liquid metal environment, but the amount of deformation observed is much less than that required for ductile cavity formation and greater than the amount usually considered necessary to initiate brittle cracks from dislocation pile-ups. This latter type of initiation model has been frequently applied to liquid-metal embrittlement. In the absence of a direct, experimental justification for it however, the validity of the approach cannot be confidently asserted unless a careful analysis is made of the ability of the metals concerned to support sufficiently large pile-ups for fracture without relief of the stress concentration by slip.

In formulating an adequate theory of liquid-metal embrittlement, an essential first step is to build up as accurate a picture as possible of all processes occurring at the crack tip. By its very nature the crack tip is very difficult to study and usually, only indirect experimental methods are available to evaluate processes occurring there.

The work described herein has been directed towards an assessment of the role of plastic deformation in both the initiation and propagation of cracks caused by liquid-metal embrittlement. The aims are best summarised in the following questions:

1. Does initiation of a crack require plastic deformation or stress alone in the presence of the liquid metal?
2. When a crack is formed does it propagate as a stable crack, requiring an increase in applied stress, during the initial stage? Does it ever in fact become unstable?
3. During crack propagation, how much plastic deformation occurs at the crack tip and what is the role of such deformation in the fracture process?

Unambiguous answers to these questions would be of great help in formulating a more adequate description if not an explanation of the liquid-metal embrittlement phenomenon. It is not known whether thermally activated processes such as diffusion and dissolution play any part in the initiation process and more precise information on the required stress and strain conditions for crack initiation is necessary. The question of stability or instability is fundamental to the whole fracture problem and an evaluation of the plastic deformation occurring during crack propagation is essential in this respect. It has usually been assumed that plastic deformation and fracture are competitive processes at the crack tip, but in a complex fracture process such as this, the possibility must be borne in mind that such deformation may be an essential prerequisite for fracture, or an integral part of a series of processes leading finally to a loss of cohesion over a small area extending ahead of the crack tip.

CHAPTER II

LITERATURE AND THEORY

Introduction

Past work on liquid-metal embrittlement may be classified into four areas:

1. Determination of the conditions of stress, strain and intrinsic mechanical properties necessary to maintain propagation of an existing crack.
2. Evaluation of data from uniaxial tensile tests to establish the effects on crack initiation of such parameters as composition, metallurgical condition, stacking fault energy and grain size of the solid metal.
3. Experiments on the nature and occurrence of delayed failure.
4. Metallographic examinations for evidence of penetration of the liquid metal prior to fracture, and direct measurement of interface energies from dihedral angle and sessile drop experiments.

It is not intended here to review all aspects of the liquid-metal embrittlement phenomenon but to examine only work in each of the four areas outlined above which has some bearing on the role of plastic deformation in the embrittlement process. Information is sought, therefore with the object of answering the question:

What is the role of plastic deformation in the initiation and

propagation of cracks caused by liquid-metal embrittlement?

Crack Propagation

Work on the propagation of an existing crack in an embrittling liquid-metal environment has been done by Westwood (1962) and Rostoker (1960). Westwood used zinc monocrystals in which a cleavage crack of a known length along the basal plane had been started, usually at liquid nitrogen temperature. Mercury was introduced into the crack and a tensile stress applied across it in a cantilever arrangement. The load at which the crack started to propagate was measured. Fracture was considered to occur when the normal stress at the crack–tip reached the theoretical cohesive strength across the basal plane. The effects of several variables on the propagation load were evaluated including the effects of relaxation at the crack-tip. Relaxation by plastic flow will result in a 'blunted' crack-tip i.e. one with the radius greater than the spacing of the cleavage planes. A blunted crack of this form was obtained by forming the initial cleavage crack at room temperature rather than at $77^{o}K$. By comparing the propagation stresses in air and mercury, Westwood deduced that the crack-tip radius controlled the elastic stress concentrating action of the crack but had no influence on the embrittling effect of the mercury. On Westwood's model the tensile stress required to propagate a crack of length C is given by:

$$\sigma = \left(\frac{E\phi}{4c}\right)^{1/2}$$

E is Young's modulus and ϕ is the product $(\rho.\eta.\gamma_o)$ where γ_o is the true surface energy of the cleavage plane, η is an environmental factor which is unity in an inert environment and ρ is a plastic relaxation factor

given by the ratio of crack-tip radius to the planar spacing.

$$\rho = \frac{a_p}{a_o}$$

For $a_p = a_o$, $\rho = 1$, giving a completely brittle, elastic crack.

Now if subscripts (1) and (2) represent different tip radii and subscripts Hg and Air indicate the appropriate test environment then we may say:

$$\left(\frac{\sigma_{Hg}}{\sigma_{Air}}\right)^2_{(1)} = \left(\frac{\phi_{Hg}}{\phi_{Air}}\right)_{(1)} = \left(\frac{\rho_1 \cdot \eta \cdot \gamma_o}{\rho_1 \cdot \gamma_o}\right)_{(1)} = \eta_{Hg} = \left(\frac{\sigma_{Hg}}{\sigma_{Air}}\right)^2_{(2)} \qquad (1)$$

(since air is an inert environment and $\eta_{Air} = 1$)

It is of interest to compare this expression and the experimental results confirming it with a theoretical expression due to Gilman (1959) relating the true surface energy and the effective surface energy for a crystal cleaved in a similar cantilever arrangement. Gilman defines the effective surface energy γ' as the sum of the true surface energy γ_s and the work of plastic deformation at the crack tip γ_p.

$$\gamma' = \gamma_s + \gamma_p$$

and γ' is equivalent to the quantity ϕ used by Westwood. γ_s and γ_p are related by:

$$\gamma_p = 9\gamma_s \ln\left(\frac{G}{\pi\tau_y}\right) \qquad (2)$$

where τ_y is the flow stress and G is the shear modulus. Using the same subscripts for test environment as above we have:

$$\frac{(\gamma')_{Hg}}{(\gamma')_{Air}} = \frac{(\gamma_s)_{Hg}}{(\gamma_s)_{Air}} \frac{[1 + 9\ln(G/\pi\tau_y)]}{[1 + 9\ln(G/\pi\tau_y)]} = \frac{(\gamma_s)_{Hg}}{(\gamma_s)_{Air}} \qquad (3)$$

which is essentially the same expression as (1) with interface energy γ_s' given by:

$$\gamma_s = \eta \cdot \gamma_o$$

Westwood's work therefore may be interpreted as an experimental verification of Gilman's theory (1959) that the true interface energy controls the amount of plastic work occuring at the crack-tip. It should be noted that Westwood's experiment measures the stress required to start a crack from the tip of an existing crack and this will be equal to the stress required to maintain crack propagation only when the tip radius of the propagating crack is the same as that radius of the stationary crack prior to propagation. In the case of cracks produced by cleavage at 77° K, this seems reasonable since the crack will be almost perfectly elastic and will relax very little when stopped. In the case of 'blunt' cracks initiated at higher temperatures however there is no way of knowing from Westwood's experiments whether the cracks propagate with blunted tips or whether a sharp crack is initiated from the blunt stationary crack. The sharp crack so produced could relax plastically at the tip when stopped, making the two cases indistinguishable through a re-propagation experiment which does not also measure the minimum stress required to maintain propagation. It is not at all certain therefore that Westwood's experiment can yield any information about plastic deformation accompanying fracture.

The question of crack-tip radius during propagation may also have important implications for the application of Gilman's theory to liquid-metal embrittlement. Gilman does not consider in any detail the effects of plastic deformation on the shape of the crack-tip and the stress distribution. It is possible therefore that the form of the relationship between

γ_s and γ_p will vary with the crack-tip radius. In this case the square bracketed terms in equation (3) would not cancel and the effective surface energies would not vary in the same ratio as the true interfacial energies. A more careful examination of the stress distributions at crack-tips is therefore needed in order to assess the compatibility of experimental results with the theory.

Rostoker (1960) performed an experiment similar to that of Westwood but the experimental technique did not permit such close control of the variables as was possible in the latter's work and the results are difficult to analyse. Rostoker's experiment was designed to measure the value of the effective surface energy during the propagation of a crack through a 70:30 brass sheet wetted with mercury. The sheet was loaded in uniaxial tension and a crack of known length was introduced by initiating a fracture at an indentation in the centre of the plate. Since the crack propagated slowly it could be stopped at any desired length by unloading and loads at instantaneous lengths during propagation could be measured visually. The applied stress to re-propagate the crack was measured and the results analysed according to the Griffith formula:

$$\sigma = \left(\frac{E\gamma'}{c}\right)^{1/2}$$

where c is the length of the stationary crack. In an experiment where only one side of the brass plate was wetted with mercury a good straight line relationship between σ and $(1/c)^{1/2}$ was obtained. Measurement of the slope gives a value of γ' of 2×10^5 ergs/cm.^{2}.indicating extensive deformation at the crack-tip. Since plastic deformation was visible to the eye on the un-wetted side, Rostoker concluded that the crack propagated

more slowly in the thickness direction than along the length. The implication is, presumably, that the large amount of plastic work is not associated with the embrittled fracture but with the inadequacy of the mercury supply. If the crack-tip runs ahead of the mercury then it will stop since the cohesive strength is higher in the absence of the liquid-metal. If the stress at the tip is increasing then plastic deformation will occur if the flow stress is reached before the mercury can catch up with the crack-tip. Rostoker tested this idea by improving the mercury supply: in a similar experiment to that above, but with mercury wetting both sides of the sheet, the stress to re-propagate the crack was found to be independent of the crack length within the accuracy of the experiment. A very low slope is consistent with an effective surface energy of the order 10^2 ergs/cm.^{2} and would seem to uphold the interpretation placed on the previous experiment. The explanation of the difference in γ' values however implies that the stress required at the crack-tip to cause fracture in the presence of mercury would be lower than the flow stress. The observed propagation stress with an inadequate mercury supply could not therefore be lower than the propagation stress for a crack of equal length with an adequate mercury supply. Within the range of crack lengths examined by Rostoker the very opposite result is observed: the propagation stress for high γ' is never greater than that for low γ'; only at the smallest crack length used, (0.25 inches), are the stresses equal, and for a crack length of 4 inches there is a difference in stresses of 28%.

From the review of the foregoing work it is evident that as reliable an assessment as possible must be made of the stress and elastic and plastic strain distributions at the crack-tip before experimental

results can be interpreted with any confidence.

Kelly, Tyson and Cottrell (1967) have recently done some theoretical work on the nature of crack-tip processes to assess the validity of current ideas on fracture mechanisms. The theory is concerned with the possibility of the occurrence of two competing processes at the tip of a perfectly elastic, smoothly closing crack. The processes are, cleavage at the theoretical cohesive stress along a crystallographic plane, and shear in a perfect dislocation-free lattice at the theoretical shear stress. In order to predict which of these processes will occur Kelly et al. have analysed the distribution of normal and shear stresses around the tip of a model crack and then calculated for given crack orientations in a variety of real solids, the ratio of the maximum normal stress across the cleavage plane to the maximum resolved shear stress on an observed slip system. This ratio, called R, is compared to the ratio of the appropriate values of theoretical cohesive strength to theoretical shear stress σ_{max}/τ_{max}. A value of R less than σ_{max}/τ_{max} indicates that if a continuously increasing stress is applied across the crack, shear at the theoretical shear stress will occur at the crack-tip before the theoretical cleavage stress is reached. If R is greater than σ_{max}/τ_{max} then cleavage at the theoretical cohesive stress will occur before the shear stress reaches the theoretical value. Due to the approximate nature of the theory, only large discrepancies between R and σ_{max}/τ_{max} are considered to be reliable predictions. Calculated values indicate that at $0^{\circ}K$, fully brittle cleavage is not expected for the face-centred cubic metals Cu, Au, Ag and Ni, or for a Lennard-Jones solid. Brittle behaviour is predicted for NaCl crystals and diamond. The results for the body-

centred cubic metals α - Fe and W predict brittle cleavage but the values of R and σ_{max}/τ_{max} are sufficiently close to give uncertainty. Since secondary factors operative in crack-tip processes have not been accounted for, the uncertainty in the prediction for body-centred cubic metals is an encouraging result in view of the ductile-brittle transition observed in the behaviour of these metals.

Comparison with observed behaviour is therefore very encouraging but in order to retain compatibility of the theory with physical reality the predictions for metals can only be tested by the behaviour of near perfect single crystals, (carefully grown whiskers, for example). In polycrystalline metals shear processes would be expected to occur well below the theoretical shear strength which therefore ceases to be the only critical shear stress to be considered. Kelly's theory was applied to the cases of copper and Cu-17Al alloy deformed in mercury in an attempt to predict the probability and extent of shear processes occurring at the tip of a propagating crack. The results and details of the calculations are given in Appendix 1. Calculations for copper have been made by Kelly et al., but the physical conditions obtaining in the liquid-metal embrittlement case differ considerably from those for which the theory was constructed. The differences are enumerated and discussed below:

1) Temperature

The calculations by Kelly et al., refer to processes at $0^{\circ}K.$, but for face-centred cubic metals the temperature effects act principally through the elastic constants and can therefore be easily accounted for. Critical shear stresses other than the theoretical shear stress are temperature dependent but have

been obtained directly from experimental, room-temperature data.

2) Cohesive strength

Kelly has used the approximate estimate of cohesive strength due to Orowan (1949).

$$\sigma_{max} = \left(\frac{E\gamma}{a_o}\right)^{1/2}$$

where a_o is the spacing of the cleavage planes, E is the appropriate Young's modulus across that plane and γ is the surface energy of the plane. In the absence of an experimentally verified mechanism for the embrittling action of liquid metals it is reasonable to assume, as does Westwood (1962), that mercury causes a reduction in the cohesive strength by an interaction with atoms in a severely strained state of bonding at the crack-tip or just ahead of the tip. Using a model of this form it is possible to make an approximate estimate of the embrittling effect by simply substituting a reduced surface energy into Orowan's formula. Precise and reliable values of the reduced surface energy are not available however a list of experimental estimates of the Cu_{sol} Hg_{liq} and $Cu\text{-}17Al_{sol}$ Hg_{liq} interface energies and other related values has been compiled and is given in Appendix 1, table A6. In view of the uncertainty in the value of γ the cohesive strength has been calculated for a range of probable values.

Orowan's estimate applies to cleavage along a crystallographic plane whereas the present case involves grain boundary embrittlement. Interatomic distances and bond strengths will vary in the grain boundary and in the presence of an embrittling liquid metal the

grain boundaries obviously possess some characteristic which makes them a preferred crack path. There is no other evidence either experimental or theoretical however which indicates that the cleavage strength of the grain boundary can be significantly less than that of the weakest crystallographic plane and in the absence of a better calculation the grain boundary cohesive strength has been taken as that for {100} for which σ_{max} is a minimum in face-centred cubic metals.

3) Crack orientation

Since the orientation of the grain boundary fracture path with respect to the adjacent crystal lattice will vary, then the resolved shear stresses upon the slip systems will also vary. To account for this the maximum and minimum values of R have been calculated. R_{min} occurs when the maximum shear stress τ_3 acts on an observed slip system. R_{max} occurs for a grain boundary on {111}, the slip system being $\{111\}\langle\bar{2}11\rangle$. The values given by Kelly et al., (1967) for plane strain conditions are:

$$R_{min} = 2/(1-2\upsilon')$$

$$\text{and, } R_{max} = 3.66/(1-2\upsilon')$$

where υ' is the appropriate Poisson's ratio.

4) Stress system

Plane strain conditions give rise to larger values than plane stress. Kelly's calculations have been based on plane strain conditions but since in the experimental work described here conditions were somewhere between the two extremes, values have been calculated for both.

5) Dislocation density

At the instant of fracture in mercury both copper and Cu-17Al are far from being dislocation-free solids, the strains at fracture being about 0.03 and 0.20 respectively. If an increasing stress is applied across a sharp crack in either of these metals in this state of strain then the maximum shear stress at the crack-tip will exceed that required to move dislocations and operate dislocation sources long before the theoretical shear stress is reached. Providing stresses at these levels act over sufficiently large volumes therefore, significant amounts of plastic deformation will occur. Elastic crack studies predict that stress falls off in inverse proportion to the square root of the distance. If a similar low index power relation holds in the case under consideration here, then problems concerned with a minimum stressed volume are not likely to arise.

A value of the shear stress required to cause plastic deformation at the crack tip cannot be defined precisely since the flow stress will not be uniform throughout the metal on a microscopic scale. Two estimates have been used: the first is the friction stress and the second is the macroscopic flow stress. The former is a measure of the stress required to move dislocations and contains a correction for work-hardening. Friction stress values have been obtained from the grain size experiments of Pargeter and Ives (1967) by extrapolating the fracture stress to infinite grain size. Only the fracture stresses for small grain sizes were used since

anomalous low values were reported at large grain sizes. The macroscopic flow stresses have also been obtained from the above authors and checked with our own results. Macroscopic flow will occur by the operation of the minimum number of dislocation sources required to comply with the crosshead motion of the tensile testing machine, and furthermore, those sources which operate will be those with the lowest values of critical resolved stress. Both of these flow stress values may therefore be underestimates. The macroscopic flow stress however is a complex quantity since compliance with the imposed strain requires that the slip occurs on at least five systems and may also require grain rotation. It is possible that these requirements may give a higher flow stress than that required for localised deformation at a crack-tip.

After due consideration to each point it was decided that the modifications necessary do not necessarily invalidate the approach and that the calculations retain their physical significance. The results are presented in tables A3 and A4. If the critical shear stress is taken as the theoretical shear strength then ductility is only predicted for pure plane stress conditions with a true surface energy of at least 300 ergs/cm.^{2}. If the critical shear stress is taken to be the macroscopic flow stress then ductility is predicted for both plane stress and plane strain conditions for a true surface energy as low as 50 ergs/cm.^{2}. When the normal stress at the crack-tip is equal to the theoretical cohesive strength of copper with a surface energy of 300 ergs/cm.^{2}, then the maximum resolved shear stress on a slip system varies from 5.25×10^{10} to 2.84×10^{10} dynes/cm.^{2} for plane stress, and from 1.67×10^{10} to 0.91×10^{10}

dynes/cm.^{2} for plane strain. The values for Cu-17Al are about 10% less. The measured macroscopic flow shear stresses must be increased by factors of 7.1 and 8.5 for copper and Cu-17Al respectively in order to reach the minimum plane strain level for cleavage, and by factors of 22 and 30 respectively for minimum plane stress level. If however we assume that the Orowan formula for cohesive strength overestimates by a factor of two or more as has been indicated by Kelly (1966) for the cases of diamond and sodium chloride crystal then the macroscopic flow stress may be quite close to the value required for fracture in plane strain. If the overestimation is no greater than a factor of two then the shear stress at the crack-tip is still higher than the observed macroscopic flow stress by a factor of more than ten for plane stress conditions. There is no calculation or measurement available at present for a more accurate determination of the cohesive strength of metals, nor is there a means of assessing the accuracy of the Orowan formula (Kelly 1966). We can only speculate therefore on the value of the flow stress at the crack-tip required to promote the conditions necessary for cleavage, bearing in mind both the inadequacy of the strength estimate and the effects on R due to changes in the shape of the crack-tip and changes in the applied stress conditons. Since fracture involves microscopic processes, the macroscopic parameters such as overall strain and applied stress are of limited value in assessing the particular conditions at the crack-tip and along the grain boundaries ahead of the crack. It is the stress and strain in the region ahead of the crack-tip immediately prior to fracture which is of importance. If the shear stresses at the crack-tip exceed the local flow stress then plastic deformation will occur ahead of the crack-tip and

the propagating crack will be preceded by a zone in which the plastic strain is greater than the uniform strain. The size and shape of this zone and the stress and strain distributions in it will be related to the crack geometry, applied stress, the constraints imposed by metal adjacent to the zone and the work-hardening characteristics of the metal. It is possible therefore that the local work-hardening of the metal ahead of the crack can raise the local flow stress at the crack-tip to a level at which cleavage becomes possible. A first step in examining this possibility is to measure the amount of plastic deformation accompanying crack propagation.

Crack velocity is also an important parameter since it will be greatly affected by plastic deformation. It is not at all certain however that the amount of plastic deformation is the controlling factor in liquid-metal embrittlement. Other factors to be considered are the kinetics of the interaction process and the mechanics of supplying liquid metal to the crack tip. Rostoker (1960) has quoted the unpublished work of two authors on crack velocity measurements, both using 2024-T4 aluminum alloy. Barclay and Rhines used a bend test arrangement in which sheets 6x12x0.125 in., were bent over a mandrel through an angle of 8° and thus held during crack initiation and propagation. The crack was initiated by applying mercury near one end of the axis of bending. It was observed that the initial crack always travelled beneath the surface of the sheet along a plane parallel with the surface. Simultaneously and at a slower rate the crack propagated perpendicularly toward the tension surface. At some distance from the liquid source the cracks failed to reach the surface; a slight depression in the tension surface indicated continued

sub-surface cracking. Velocities were measured with both cine photography and electrically conductive strips. Measuring up to crack lengths of six inches it was found that the crack velocity was inversely proportional to the crack length and was only 1 in./sec. after propagating one inch. In similar experiments however where the entire crack path was wetted with mercury, the velocities seemed to lie between 50 and 200 in./sec. indicating that the velocity is in some way associated with the mercury supply rate. Rostoker (1960) also quotes a value from unpublished work by Otto in which strips of 2024-T4 aluminum, 3 in. wide, were stressed in uniaxial tension and embrittled: when the mercury supply was applied only at one point the observed velocity was 300 in./sec.; higher velocities were observed when the entire width was wetted with mercury. These are higher than recorded by Rhines and Barclay but this could be due to the different stress systems imposed. In an experiment on embrittlement of annealed brass sheets, 0.02 in. thick, loaded in uniaxial tension and embrittled by mercury, Rostoker (1960) states that load versus crack length measurements could be made visually. The sheets had a gauge length of 6 in. and a width of 12 in. An indentation in the centre of the sheet initiated the crack which spread towards each edge along a band wetted with mercury. The experiment was not intended to measure crack velocity, but an order of magnitude assessment can be made if it is assumed that the minimum time for propagation across the whole width was one second. This seems reasonable since visual measurements of instantaneous crack length would require at least this amount of time. The maximum velocity is therefore 6 in./sec., considerably less than that for 2024-T4 aluminum even though the entire crack path was wetted with mercury. Two important differences should be

noted between this last result and those for the aluminum alloy:

1. The aluminum alloy was age hardened whereas the brass was single phase and annealed. The stored elastic energy per unit volume will no doubt be greater in the higher strength aluminum alloy than in the brass and the availability of energy may influence the crack velocity. The difference in mechanical properties between the alloys may also control the amount of deformation which either occurs as a competitive process to the fracture or is necessary to raise the local flow stress to a critical value. In either case the velocity is likely to be affected.
2. The brass sheet was only 0.02 in. thick compared to 0.125 in. for the aluminum alloy. The stress conditions at the crack-tip are nearer to plane stress in the brass sheet which may therefore be expected to show greater ductility.

Crack velocities in brass have been measured by Rhines and Barclay in unpublished work quoted by Rostoker. The tests were similar to those performed for 2024-T4 aluminum with a localised source of mercury. Velocities of the order of 3 in./sec. are reported. The same authors have observed effects due to the temperature and hydrostatic pressure of the mercury supply that furnish very strong evidence that the velocity is controlled by the rate of supply of liquid metal.

It should be noted that even the highest velocities recorded are far less than those measured for brittle fracture in steel or glass which are of the order of 6×10^4 inches per second compared to a maximum recorded value of 3×10^2 inches per second in liquid-metal embrittlement.

If supply rate of liquid metal is the controlling factor then there are some important implications concerning the nature of the crack-tip. An unstable crack, i.e. one which will continue to propagate without an increase in the applied load, will move stepwise through the specimen, ceasing to propagate each time that the liquid metal supply becomes insufficient. The stresses at the tip will cause plastic deformation to occur until the stress concentration is relieved or until more liquid metal is able to move into the crack-tip and conditions for cleavage are re-established. Such deformation is not a part of the fracture process and competes with cleavage for the elastic energy stored in the stressed system. The extent of this deformation will depend on the stress concentration at the crack-tip and on the extent to which the liquid metal supply is capable of keeping up with the crack. The shape of the crack will thus be very important: if plastic deformation occurs at the crack-tip in spite of an adequate liquid metal supply then the additional deformation will be less important than in the case of an atomically sharp, elastic crack. Moreover, a blunted crack will present less impedance to the supply of liquid metal to the tip than a sharp crack.

If the crack is stable it will propagate only as long as an applied strain rate or loading rate is maintained, and the amount of deformation occurring at the crack-tip when there is insufficient liquid metal will be a function of the rate of straining or loading.

High velocities, comparable to those reported for 2024-T4 aluminum, have not been observed in brass; a general effect of velocity control through liquid metal supply rate cannot be established therefore without first distinguishing between effects due to differences in mechanical

properties. It is sugnificant to note that in thin brass sheet with an adequate mercury supply, the velocities are no higher than with a localised mercury source. The observation by Rhines and Barclay that crack velocities in the surface layers of a bent aluminum alloy plate was slower than in the interior is also important. The tensile stresses are greatest at the surface and there is no reason to assume that the rate of mercury supply at the surface is any slower than in the interior. Although the tensile stress is greatest at the surface it is possible that the stress conditions close to the surface are much nearer to plane stress than in the interior. There is some evidence therefore that under plane stress conditions plastic deformation may be the rate controlling process even with an adequate supply of liquid metal.

In summarising the crack velocity work, there is substantial evidence that the liquid metal supply rate is the controlling process but the picture is somewhat confused by other factors such as metallurgical condition and stress system.

Crack Initiation

It has usually been assumed in liquid-metal embrittlement studies, as it has in the past for general brittle fracture theory, that crack initiation is the controlling process. Most theories for the initiation of cracks in an embrittling liquid metal environment have accordingly been based on mechanisms developed to explain micro-crack formation in body-centred cubic and close packed hexagonal metals. There are some difficulties in justifying this approach to liquid-metal embrittlement, particularly where face-centred cubic metals are concerned, since these metals are not

intrinsically brittle and have usually been observed to fracture only after a considerable amount of plastic deformation has occurred. There are a number of reasons however why the approach to initiation has been closer to that for brittle metals than that for a process such as stress-corrosion cracking; in particular, attempts to detect significant corrosive activity or penetration prior to fracture have usually been unsuccessful, and the effect of increasing the grain size which can induce a ductile-brittle transition in body-centred cubic metals, causes a reduction of fracture stress in the liquid-metal embrittlement of face-centred cubic metals.

Westwood (1965), has observed that the prerequisites for liquid-metal embrittlement would seem to be,

(i) some measure of plastic deformation,

(ii) the existence in the specimen of a stable obstacle to dislocation motion serving as a stress concentrater.

(iii) adsorption of the active embrittling species specifically at this obstacle, and subsequently at the crack-tip.

From his work on zinc monocrystals and asymetric bicrystals, Westwood concludes the following:

(i) Carefully prepared and handled zinc monocrystals oriented for single slip and tested in tension are not embrittled by mercury or gallium unless these liquid metals are adsorbed specifically at kink bands formed during deformation in the vicinity of the grips.

This conclusion contradicts an early piece of work by Likhtman and Shchukin (1958) and Shchukin, Pertsov and Gorynov (1959) who have reported that

zinc monocrystals oriented for single slip can be significantly embrittled by liquid mercury or gallium. Westwood has concluded that the results obtained by these workers have been complicated by grip effects which have given rise to kink band, crack initiation sites. Westwood's own work indicates that deformation alone is not sufficient to cause fracture and that stress concentration at some stable obstacle to slip is also required.

(ii) Experiments on the cleavage fracture of amalgamated asymetric bicrystals provide convincing support for the theoretical criteria for cleavage fracture in zinc proposed by Likhtman-Shchukin (1958) and derived from an analysis by Gilman (1958).

This fracture model assumes that the critical process is the opening up of a basal slip plane into a microcrack when a sufficient number of dislocations are piled up under an applied shear stress against a stable obstacle. The criteria for fracture involve shear stress along the slip plane, normal stress across the plane and the surface energy. In the case of fracture in mercury the mechanism obviously requires the intersection at the mercury wetted surface of the stable obstacle and the slip plane containing a dislocation pile up of sufficient size. The effect of the liquid metal is apparent through the reduced surface energy and Westwood has proposed that the underlying atomic process is a stress induced adsorption of liquid metal atoms at the site of stress concentration similar to that which subsequently occurs at the crack-tip.

Very similar theories have been proposed for crack initiation in face-centred cubic metals embrittled by a liquid metal. These have been

based on the models proposed by Petch (1953) and Stroh (1957) for fracture of body-centred cubic metals. Analyses of the liquid-metal embrittlement phenomenon based on fracture models of this type have been made by Rostoker (1960), Rosenberg and Cadoff (1963), Johnston, Davies and Stoloff (1965) and Pargeter and Ives (1967). Essentially, the fracture occurs when an array of dislocations, piled up at the intersection of a grain boundary with the wetted surface, exerts sufficient stress that the opening up of a crack in the adjacent grain results in an overall decrease in energy. Stroh's (1957) analysis indicates that in the absence of plastic flow such a crack will be unable to find an equilibrium position and so will spread catastrophically. Crack initiation is assumed to be the critical process.

As in the case of stresses at a crack-tip it is necessary to consider the possibility that the stress concentration at the head of the piled-up dislocation array will cause slip to occur before the normal stress reaches a sufficient level to open up a crack. Stroh (1957) has presented an analysis for steels where fracture occurs at yield and the applied stress may be less than that to operate Frank-Read sources still pinned by solute atmospheres. The problem of an inadequate supply of unpinned dislocation sources will not occur in face-centred cubic materials deformed well beyond macroscopic yield. However, even when the applied stress is equal to the macroscopic flow stress, not all sources will operate due to back stress effects from pile ups and orientation effects. The problem of crack initiation is a microscopic one and the effect of the stress concentration at the head of a pile up at a grain boundary on a source in the next grain will depend upon the number of slip

systems available, orientation of the source with respect to the pile up in the adjacent grain and the nature of other stresses acting on the source from dislocation arrays. It is possible therefore that situations may arise where the stress concentration at the head of a pile up builds up to the level where crack formation can occur before neighbouring dislocation sources can be operated. Davies, Johnston and Stoloff (1965) consider this to be the case in copper solid solution alloys embrittled by mercury and in an ordered body-centred cubic Fe-Co alloy which fractures in a brittle fashion after several percent deformation. No detailed analysis has been given to show that the model is valid but there is a considerable amount of favourable evidence in the effects of grain size and stacking fault energy. Bigger grain sizes permit pile-ups containing larger numbers of dislocations and hence larger stress concentrations. Low stacking fault energy and ordering impede cross slip; dislocation pile-ups therefore become more coplanar and cause greater stress concentrations. Predicted effects of grain size are reported by Pargeter and Ives (1967), Rostoker (1960) and Rosenberg and Cadoff (1963). Stacking fault energy effects have been found by both of the above and also by Johnston, Davies and Stoloff (1965). Values of the effective surface energy appropriate to the initiation process can be derived from the grain size effect. Some typical values are given in table A6b. The values correspond to the expected magnitude of the true surface energy indicating that very little plastic deformation occurs at the crack-tip during the initiation phase.

The effects of metallurgical condition upon the susceptibility to liquid-metal embrittlement have been studied quite extensively. It is generally concluded that in any given metal or alloy, raising the yield

stress by ageing or pre-straining will increase the susceptibility. This quantity is generally measured in terms of the strain at fracture or the ratio of fracture stress to yield stress. It should be borne in mind that these macroscopic parameters are being used to define the critical conditions for a microscopic process; they must be used with some caution. The effects of pre-strain are of particular interest. Rosenberg and Cadoff (1963) measured the fracture stress of α- brass with mercury as a function of the pre-strain in air. They observed that after about 30% pre-strain the fracture stress is lower than the pre-stress and since they report that no relaxation occurred during unloading from the pre-stress level, it must be concluded that fracture occurred in mercury without measurable plastic deformation. These authors observed that deformation in the presence of mercury must have damaging effects over and above those due to equivalent deformation in air since the pre-strain in air necessary to cause an elastic fracture during subsequent reloading in mercury, was greater than the normal fracture strain for deformation in mercury without pre-strain.

Delayed Failure

Delayed failure of metals exposed to an embrittling liquid metal has been widely reported. The important aspects of this phenomenon are brought out in the following questions.

1. Can fracture occur if no plastic deformation takes place during the period of exposure?
2. Must a finite time of exposure elapse before fracture occurs? i.e. Can fracture be instantaneous upon wetting with the

liquid metal?

The only direct attempt to show that deformation does not always occur was made by Nickols and Rostoker (1965) who applied a micro-creep transducer to a tensile specimen of aged Cu-2%Be alloy held at constant load and wetted with mercury. No measurable plastic deformation occurred before fracture. The elastic fracture after large pre-strains reported by Rosenberg and Cadoff (1963) and mentioned in the last section is also an example of fracture without prior plastic deformation.

Indirect evidence for fracture without deformation is also obtained in experiments seeking to answer the second question. Bryukhanova et al., (1962) reported "instantaneous" failure of zinc polycrystals when held at 1000 gm./mm.^{2} and wetted with mercury. "Instantaneous" failure at stresses less than the macroscopic yield stress have also been reported by Nickols and Rostoker (1965) for aged Cu-2%Be alloy, and by Rostoker (1960) for aged 2024-T4 aluminum alloy. It must be remembered that the term "instantaneous fracture" used by these authors refers only to the fact that the delay time was smaller than could be measured. The application of the liquid metal takes time, especially if a mercurous salt solution is applied first, and it is difficult to know exactly when wetting occurs.

The answers to the two questions above are of immense importance to any crack initiation theory. Pile up models such as those proposed by Johnston et al., (1965) and Westwood and Kamdar (1965) are best able to explain instantaneous fracture but further explanation of the need for a lengthy exposure time at lower stresses is then required. Stress aided and thermally activated processes such as diffusion, dissolution and grain

boundary penetration are most suited to an explanation of the relationship between the stress level and the exposure time required for fracture, but it would be difficult to explain a truly instantaneous faioure along these lines.

Metallographic Evidence for Penetration

Attempts to detect cracks prior to fracture have in the past been largely unsuccessful. Rinnovatore et al., (1966), however have succeeded in showing that when aged Cu-2%Be alloy is held at constant stress and exposed to mercury, surface cracks form at grain boundaries prior to the delayed failure. Furthermore, the authors showed that the average length of these cracks increased with both time and stress level. It seems probable that it is one of these growing cracks which finally caused fracture. Levine and Cadoff (1964) also detected cracks prior to failure in a Cu-4Ag alloy wetted with mercury and deformed in uniaxial tension. The technique used by these authors was to wet the specimen with mercury, load it in tension to a stress less than the expected fracture stress, then unload and remove the mercury by heating under vacuum. Examination of the surface revealed that a crack 0.1mm. in length had formed at a stress which was only 80% of the fracture stress. The specimen was re-wetted with mercury then loaded to a slightly higher stress, unloaded and examined. This procedure was repeated until fracture occurred. It was observed that the number of surface cracks increased with the stress level and that the final fracture occurred by the linking up of some of the cracks. The authors reported that the cracks observed at one stress level did not usually increase in size when the stress was raised. This may be construed

as evidence that cracks are formed quickly and either propagate quickly to complete failure or under less favourable conditions soon stop growing and remain static. Some cracks were observed to link up before fracture however, and it is possible that the technique used to remove the mercury contaminated the crack-tips, especially at the surface, and so prevented wetting when mercury was applied. The existence of cracks prior to failure did not appear to affect the stress-strain curve.

Work on measurements of dihedral angles for solid metal/liquid metal interfaces can also be informative. Interest in the dihedral angle followed the work of Smith (1953) who suggested that grain boundary penetration and embrittlement could occur when the dihedral angle was zero. McLean (1957) had modified this to include the effects of stress by postulating that where the angle is greater than zero, penetration can only occur if an applied stress does work against the atomic cohesion across the boundary. There is little data availahle to check this criterion thoroughly. Rogus (1966), however, has shown that the dihedral angle between polycrystalline copper and a Bi/Tl liquid alloy decreases as the thallium content decreases; this corresponds well with Morgan's observation (1954) that the susceptibility of copper to embrittlement by this liquid alloy increases as the thallium content decreases. Also of interest is an observation by Waterhouse and Grubb (1962) that stress has no effect on the dihedral angle between molten lead and brass or copper, and that there is no effect on the rate of approach to the equilibrium angle.

Considerably more reliable data is necessary however to assess the penetration criterion.

CHAPTER III

EXPERIMENTAL PROCEDURES

GENERAL

All experimental work described herein was performed on Cu-17 at. % Al, solid solution alloy. The alloy was made up from 99.99% copper and 99.999% aluminum and vacuum cast in graphite molds. The ingots were reduced to wire form by a combination of cold rolling and drawing with intermediate anneals in hydrogen where necessary. All subsequent annealing operations were done in 1 atm. of argon. Two diameters of wire were used, 3 mm. and 1 mm., with grain sizes of approximately 0.03 mm. and 0.08 mm. respectively. The use of such narrow wires for fracture work is in some ways undesirable but in liquid-metal embrittlement work there is an advantage in small cross sections since the risk of effects due to an insufficient supply of liquid metal is minimised. Prior to testing all specimens were electropolished in a mixture of methanol and nitric acid to obtain smooth surfaces. Wetting with mercury was accomplished by first applying a solution of mercurous nitrate which deposited a thin film of mercury; bulk mercury could then be applied.

Mechanical tests were performed using an Instron tensile testing machine. For uniaxial tensile tests the wires were held in self aligning split grips. The specimen surface in the vicinity of the grips was left free of mercury to avoid spurious effects. All tests were performed at room temperature and in every case, immediately following the application

of mercury.

Whenever it was necessary to move mercury from a specimen, this was accomplished by heating to 200°C. for 10 minutes in argon at a pressure of less than 1×10^{-4} torr.

DETERMINATION OF PLASTIC DEFORMATION ACCOMPANYING FRACTURE

Two techniques were used to assess the amount of plastic deformation accompanying crack propagation. These were, micro-hardness and X-ray line broadening. Specimens from the same batch were used in both experiments. Fracture surfaces were produced by deforming mercury coated wires of 3 mm. diameter in uniaxial tension. The grain size was approximately 0.04 mm., and the strain rate was 0.05 per minute.

The experiments were designed to give estimates of three quantities:

1. The flow stress at the tip of the propagating crack.
2. The distribution of plastic strain about the crack.
3. The energy of plastic deformation per unit area of crack surface.

Micro-hardness

After removing the mercury, the fracture surface was electroplated with copper, mounted and sectioned longitudinally. The specimen was then carefully ground and polished to expose the maximum thickness section for examination. Since surface condition is important in micro-hardness testing, the surface was prepared carefully by alternate polishing and etching, finally using 0.3 micron vibratory polishing followed by a light etch in an aqueous solution of potassium dichromate and sulphuric acid. The micro-hardness tests were performed on a Wilson Tukon hardness tester using a

136° included angle, diamond pyramid indenter and a load of 25 gm. The hardness was measured as a function of distance from the fracture face by taking the mean of groups of at least 25 measurements made at various distances. Each group of indentations traversed the width of the specimen. Indentations were made in the centres of grains, the diagonal length being about half the grain diameter. Even without copper plating there appeared to be no changes in hardness at the extreme edges of specimens which had been uniformly strained. The plating on the fracture surface therefore served as an additional safeguard ensuring that edge effects did not confuse the results.

The indentation test itself produces a deformation of 8 to 10 per cent. Since the changes in strain which were to be measured could be less than this amount, it is pertinent to ask whether or not the technique is capable of detecting such small changes. Data presented by Tabor (1950) for diamond pyramid hardness tests on polycrystalline copper in various stages of pre-strain indicates that the test is quite sensitive to small changes in strain. The hardness number increased from 58 to 69 for a change from 6 to 12.5 per cent of pre-strain. The hardness number is a calculated pressure which is related to the flow stress of the material around the completed indentation by a constant ratio. Sensitivity to changes in the initial strain in the material is therefore dependent upon the work hardening rate. At low strains, Cu-17Al work hardens at the same rate as copper and at a higher rate after about 0.05 strain. Adequate sensitivity was therefore expected, provided that a statistically significant number of readings was made.

In order to facilitate analysis of the results a series of stan-

dards was prepared. Wires from the same batch as the fracture specimens were deformed by known amounts in tension and the hardness values determined as a function of initial strain and flow stress using the same procedure as before. The calibration curve of micro-hardness versus flow stress is given in figure 5. Values of strain may be obtained from the appropriate stress-strain curve. The hardness values from the fracture specimen may therefore be converted into equivalent values of uniform strain. The relationship between plastic deformation around a propagating crack and that in a slow tensile test is discussed later.

X-ray line broadening

Plastic deformation of a metal can give rise to diffraction line broadening by decreasing the effective crystallite size through cell formation, by creating non-uniform elastic strains in the lattice and by increasing the density of planar faults such as stacking faults and twins. Since Cu-17Al has a very low stacking fault energy, dislocation arrays tend to be coplanar and line broadening would be expected more from planar faulting than from cell formation.

The technique used was similar to that reported by Felbeck and Orowan (1955). Mercury was removed from the fractured wire which was then mounted in a Phillips X-ray diffractometer so as to give a back-reflected beam from the fracture surface. For a given reflection line therefore, information was contributed to the diffracted beam by all crystallites within the penetrated layer which were oriented correctly for that reflection. The line profile was traced out by automatic chart recorder using a goniometer scanning speed of 1/8° of 2θ per minute. Copper K_α radiation was used with a nickel filter to reduce K_β intensity. The counter was a

self-quenching, krypton gas, Geiger tube. Primary and reflected beam slits were 1° each with a 0.006" aperture placed behind the filter. The entire fracture surface was irradiated. Choice of radiation was determinied by two factors: first the diffracted intensity must be sufficiently high to give a good peak-to-background ratio, and secondly the penetration depth must be minimised as far as possible. Low penetration was desirable since excess plastic strain might fall off rapidly with distance from the fracture surface and a highly penetrating beam would therefore average information from regions with widely different states of plastic deformation. Fe-K_α and Co-K_α radiations are both highly absorbed by copper and have very low penetrations but the intensities were found to be too low. A satisfactory compromise was found in using Cu-K_α radiation. Back reflection from {111} was used since the diffracted beam had a high intensity, and a small penetration depth due to the low incident angle. Stacking faults in dissociated dislocations in face-centred cubic metals lie on {111} . Use of this reflected beam therefore utilises faulting information from three of the four {111} glide planes.

A calculation of the depth of penetration of Cu-K_α radiation at the {111} incidence angle, into Cu-17Al alloy shows that 95 percent of the total back-reflected intensity comes from within 0.013 mm. of the surface, which is certainly a low enough penetration for the present purpose.

The variation of plastic strain with distance from the fracture surface was obtained by chemically polishing back the surface in a 50 per cent solution of nitric acid and obtaining diffraction line profiles at various depths. The polishing depth was calculated from a separate dissolution rate experiment.

The parameter measured from the line profiles was the line width at the "half-area height". This quantity was obtained by measuring the length intercepted by the line profile on an abscissa which bisected the area under the profile. It was considered preferable to use a width parameter which did not require measurement of the maximum line height since the extreme peak may sometimes be cut off when using an automatic scanning technique. The area under the profile was measured with a planimeter taking care to account for the long tails when drawing in the base line at the background level.

The technique used to obtain the profiles was not sufficiently accurate to warrant a rigorous analysis. The line widths were therefore converted into equivalent values of plastic strain by comparison with standards. These were produced by deforming identical tensile specimens to known strains, cross-sectioning by spark cutting and chemical polishing to remove cutting damage, then obtaining a diffraction line profile from the sectioned face. A calibration curve of line width versus equivalent uniform strain was constructed(figure 4).

Analysis of micro-hardness and X-ray results

In attempting to estimate the three required quantities, flow stress, plastic strain and work of deformation, calibration curves have been used. These curves (figures 4 and 5) have been obtained from uniaxial tensile tests at low strain rates and the effects of the widely different modes of deformation must be considered.

1. Stress system

Kelly et al.(1967) have analysed the stress distribution about a crack and conclude that a state of biaxial tension will

exist at the tip. Plastic strain accompanying fracture therefore occurred under a biaxial stress system whereas the standards were deformed in uniaxial tension. Except in the limiting case of plane stress there will be some constraint against strain perpendicular to the biaxial stress plane. This implies some degree of triaxiality and the ratio of maximum principal stress to maximum shear stress will be increased. In the limit of pure plane strain the ratio will be increased by $1/(1-2\upsilon)$, where υ is Poisson's ratio. Taking $\upsilon=0.38$ for Cu-17Al, the maximum normal stress at the crack tip will be greater by a factor of 4 than the corresponding stress in uniaxial tension for the same shear flow stress.

2. Stress distribution

Unlike the macroscopically uniform stress field in a uniaxial tensile test the stresses around a crack tip will vary considerably. On a microscopic level however the stresses acting on dislocations and dislocation sources in a polycrystal are always non-uniform. Since the macroscopic stress distribution around the crack will probably vary with the inverse square root of distance, the range over which significant changes occur may be large compared with the range of these microscopic stress variations which will exercise the dominant effect.

3. Strain rate

Face-centred cubic metals are not very sensitive to changes in strain rate but the effects must be accounted for. The strain rate during fracture will be very much higher than

in the standard tensile tests and this will have the effect of raising both the flow stress at a given strain and the energy of plastic deformation required to achieve that strain. An estimate of the strain rate in fracture can be obtained as follows. Felbeck and Orowan (1948) found that deformation extended to about 0.5 mm. below the crack surface. If it is assumed that the deformation zone also extends 0.5 mm. ahead of the crack then for a total strain of 0.20 and a crack velocity υ the strain rate is $(0.20 \times \upsilon)/0.5$. Taking a velocity of 3 inches per second for brass fractured in mercury, reported by Rostoker (1960), the strain rate is 1800.0 per minute. The highest strain rate for which it was possible to obtain a stress-strain curve from the testing machine was only 30.0 per minute. By using a very low strain rate (0.0016 per minute), however, the effect of four orders of magnitude change was measured. An estimate was then made for the change due to an additional factor of 60 in the strain rate. The measured and estimated stress-strain curves are shown in figure 3.

Since the flow stress and work-hardening rate are not drastically altered by changes in strain rate and since the strains around the crack are not expected to be greater than 0.30, then it is reasonable to assume that the dislocations substructures produced by a given amount of strain will be basically the same for slow uniaxial tensile deformation and rapid deformation at a crack tip. The X-ray technique gives a direct measure of the dislocation substructure and the micro-hardness tests give an

indirect measure, since the flow stress is related to the substructure. Plastic strain is therefore the parameter giving the most reliable correspondence between the standards and the fracture specimens. The microhardness tests measure flow stress at low strain rate and the corresponding strains for the standards have been obtained from the low strain rate curve. Values of plastic strain for the fracture specimens have therefore been obtained for low strain rates. Values of shear flow stress and work of deformation corresponding to these strains must be taken from the estimated, high strain rate curve in figure 3. Some adjustment for triaxiality of the stress system must be made in calculating normal stresses at the crack tip and the work of plastic deformation. This latter quantity is given for any strain level by measuring the area under the stress-strain curve at that strain. The area represents energy per unit volume and the values obtained for uniaxial tensile deformation at a strain rate of 1800.0 per minute are shown in figure 6. From the plastic strain distribution at the fracture face (figure 1), an equivalent curve may be drawn for specific energy of plastic deformation versus depth below the surface. The area under this curve gives a direct reading of the energy of plastic deformation per unit area of the fracture surface, (figure 2).

CRACK VELOCITY MEASUREMENTS

Crack velocity can give a useful indication of the nature of rate controlling processes at the crack tip. Great caution must be used however in interpreting the results of such an indirect evaluation of crack-tip processes.

The measurements made in the present work were only approximate

estimates to serve as an order of magnitude guide to the rates of crack tip processes. Velocities were measured by observing the rate at which the load fell off during crack propagation. The load was measured by the Instron load cell which gives a nearly instantaneous recording. The limiting factor is the response of the pen recorder. By using 1 mm. diameter wires however, and a high load recording range it was possible to obtain recordings well within the limit of response. The specimens were strained at a low rate of .002 per minute and the chart speed was set at 50 in./min. Great care was taken to ensure that the mercury supply was adequate. When the entire gauge length was wetted it was noted that the mercury tended to collect at the bottom of the wetted band leaving only a thin film at the top. To avoid this uneven distribution, several very narrow wetted bands were used instead of a single wide band. In order to obtain a velocity measurement it is necessary to assume that during crack propagation the stress across the unbroken section remains constant. Since the Instron is a constant strain rate machine and the strain rate was low this seems to be a reasonable approximation for an order of magnitude calculation. The velocity obtained has units of area/time and some assumption about the width of the crack front must be made to obtain a linear velocity.

Estimates of this kind were made for specimens in annealed and prestrained initial conditions. Crack velocities were also measured for fractures in notched bend tests. Since the prestrain condition of the metal ahead of the crack will vary continuously in magnitude and will change in sign, it was thought that these tests might give some indication of the factors controlling crack velocity.

METALLOGRAPHIC EXAMINATION OF THE FRACTURE SURFACE

As a further aid to deduction of the fracture mechanism the fracture surfaces were optically examined after removal of mercury. The roughness of the surface made replication difficult but by annealing 3 mm. diameter rods to give large grain sizes of about 0.5 to 1.0 mm., direct optical examination was possible at magnifications up to x150.

PRESTRAIN EXPERIMENTS

The effects of prestrain are informative in assessing the applicability of critical conditions for the onset of fracture. The following questions were examined in this work:

1. At what level of prestrain in air will fracture occur in the elastic region when the specimen is subsequently wetted with mercury and re-loaded?
2. What are the effects of compressive prestrain in air relative to tensile prestrain?
3. What are the effects of compressive prestrain in mercury relative to tensile strain?
4. Under what conditions of prestrain will delayed failure occur?

All prestrain work was done on 1 mm. diameter wire with a grain size of 0.08 mm. The work related to question 1 above was done in uniaxial tension at a strain rate of 0.05 per minute. Specimens were prestrained in air, unloaded, wetted with mercury then re-loaded to fracture.

The experiments concerned with questions 2 and 3 were performed using a combination of bend and uniaxial tension tests. Wire specimens were first bent to various radii of curvature and annealed. With the ends

held in self aligning split grips the bent wires were pulled straight in the Instron and then strained uniaxially to fracture. The initial bending and annealing produced a grain size variation across the section which was found to be symetrical across the neutral plane.

During straightening the concave side was deformed in tension and the convex side in compression. The degree and sign of strain therefore varied across the section with maximum values at the intersection of the specimen surface with the plane of bending. After straightening both sides were placed in tension but with prestrains of opposite sign. The magnitudes of the prestrains will be similar if the compressive and tensile yield stresses are the same.

Four types of test were performed:

1. Mercury applied to the convex side before straightening.
2. Mercury applied to the concave side before straightening.
3. Mercury applied after straightening to the side prestrained in compression.
4. Mercury applied after straightening to the side prestrained in tension.

The final uniaxial tensile test was always performed with mercury on one or other side of the wire. Fracture will not occur in compression but if damage due to deformation in air or mercury occurs prior to fracture then this combination of tests may establish whether or not such damage is dependent on the sign of the deformation.

Three radii of bending were used, giving maximum strains in bending of 0.026, 0.047 and 0.080. Five specimens were performed for each bend radius and type of test. The observed values were stress at fracture

and the uniaxial tensile strain at fracture measured from the point of straightening. The strain is referred to the length of the specimen at this point. A schematic load versus elongation curve is shown in figure 9.

The question of delayed failure is related to some unpublished work by Pargeter and Ives in which the relationship between time-to-failure and stress level was examined for Cu-Al alloys. The tensile specimens were loaded in air then held at constant load and wetted with mercury. The aim of the present work was simply to ascertain whether or not delayed failure would occur at constant strain.

DETECTION OF SURFACE DAMAGE

Direct evidence for damaging activity due to the mercury, occurring well before fracture was obtained in the following way. Wires of 1 mm. diameter were wetted with mercury and strained in tension to a strain which was about 0.7 of the known fracture strain for this material. The specimens were then unloaded and after removal of mercury a measured amount was electropolished from the surface. Mercury was re-applied to the surfaces and the specimens were deformed in tension to fracture. To evaluate the effect of the electropolishing treatment two standard tests were performed both following the same loading, unloading and re-loading sequence. In the first test the mercury was not removed after unloading and so retained all of the damage caused by the initial strain in mercury. In the second test the initial strain was carried out in air, and mercury was applied only after unloading. When the final loading to fracture commenced therefore, these specimens bore no damage at all due to deformation in mercury. The fracture stresses and strains were measured and those for the electro-

polished specimens were compared with the two standards. Various electropolishing times were used in order to estimate the depth of damage. Each test was performed on five specimens and mean values were calculated. The test sequences are shown schematically in figure 10. Two batches of specimens were used; these had slightly different grain sizes and the fracture stresses and strains therefore differed. Since the experiment is a qualitative demonstration only it was considered justifiable to combine the results for the different batches by normalising to unity the fracture stress and strain differences between the two standard experiments. The results for the electropolished specimens are therefore presented in terms of fractional recovery from the 'total damage' state to the 'no mercury-damage' state.

A metallographic examination for the existence of cracks was also carried out by using double-notched specimens deformed in uniaxial tension and in four-point bending. The notches were machined in 3 mm. diameter wires and were 0.5 mm. deep with rounded tip radius of about 0.1 mm. Mercury was applied to the notches and the wires were deformed to fracture. Sectioning and metallographic examination were then performed to detect the presence of cracks at the notch which had not fractured. In same bend tests the notches were placed on the compressive side. Fracture did not occur but after considerably greater strain than that required for fracture in tension the wires were unloaded and the mercury was removed from the surface. The wires were then straightened so that the notches would deform in tension and any incipient cracks present would open up. A metallographic examination followed as before.

CHAPTER IV

RESULTS

Plastic deformation at the fracture surface

The variation of X-ray line width with depth below the surface is given in table 1 for two fracture specimens, E_2 and E_6. Equivalent strains and specific energies of plastic deformation have been calculated from the standard calibration curve in figure 4 and from the high strain rate curve in figure 3 respectively; the results are given in figures 1 and 2. A single measurement at the fracture face of a third specimen E_{12} is also included in figure 1.

Micro-hardness variations are presented in table 2 and the standard calibration of micro-hardness and flow stress is shown in figure 5. . Micro-hardness values at the fracture surface have been converted to flow stress through the calibration curve and then to equivalent plastic strains through the low strain rate curve in figure 3. Equivalent specific energies of plastic deformation have been calculated from the high strain rate curve. The variations of these two equivalent quantities are presented in figures 1 and 2 respectively. The curves are drawn for specimen E_7 and two points have been inserted in figure 1 for specimen Z_{11} for which the crack velocity was also measured.

The results from the two techniques are basically similar. Plastic strains in the range 0.15 to 0.25 are recorded at the fracture surface. The micro-hardness tests record a lower strain than the line broadening

in X-ray diffraction. Each micro-hardness test gives an average reading over a distance of 0.04 mm. from the surface, the indentation itself extending from 0.01 to 0.03 mm. depth. The reading gives an average for the grain adjacent to the surface. X-ray diffraction however derives 75 per cent of the information in the reflected beam from a depth of 0.006 mm. and will therefore measure variations in substructure within a single grain. A higher reading would therefore be expected from the X-ray results.

From the high strain rate curve in figure 3 the shear flow stress at the crack tip is estimated to reach a maximum value between 25 and 35 Kg/mm^2.

At greater distances from the surface the X-ray results indicate larger deformations than the micro-hardness tests. It is difficult to ascertain whether the differences are due to real variations between the three specimens or due to spurious effects. The micro-hardness technique is less susceptible to such effects than the X-ray method and more confidence has been placed in the figures derived from the former technique. Energies of plastic work are of the order of 10^9 $ergs/cm^2$ and the depth of the plastic strain zone accompanying the crack is about 0.7 mm. Exact figures are given in table 3.

Crack velocities

Chart traces of load versus time during fracture are shown in figure 7. Figure 7a refers to 1 mm. diameter wires deformed in uniaxial tension and figure 7b refers to notched bend tests in 3 mm. diameter wires. The maximum slopes for the tensile specimens are similar for annealed and prestrained conditions. The oscillating load in the slow tail of the curve

indicates alternate predominance of work hardening and crack propagation. Assuming that the crack velocity is proportional to the rate of load change and assuming a crack-front width of 0.7 mm., the maximum velocities are both of the order of 10 mm./sec., but the tail-off in crack velocity occurs at a higher load in the annealed specimen.

The notched bend tests indicate slower rates of crack propagation. For crack fronts 2 mm. wide the maximum slopes give crack velocities of 1 and 6 mm./sec. for annealed and pre-strained specimens respectively. It is important to note that when a slight difference in cross sectional area is accounted for, the applied stresses at fracture are identical for annealed and prestrained specimens. This would be expected since the small plastic hinge area at the notch is the only region which has yielded. The remainder of the wire is deformed elastically and the prestrain of 0.06 would not be expected to affect greatly the applied stress required to cause plastic deformation at the notch. The significance of the equal applied stresses is that the total stored elastic energy available to the propagating crack will be equal in each case and differences in crack velocity cannot be attributed to differences in available energy. The tail-off to low rate of load change occurs at a slightly lower load in the prestrained wire. At this stage in the fracture the wire appeared to consist of two straight arms joined by a sharp angled plastic hinge.

In separate notched bend test experiments it was noted that if the crosshead motion was halted in the rapid load change region, the load continued to fall off at an apparently unchanged rate until the tail-off region was reached when crack propagation slowed very rapidly and soon stopped completely. It was found that the crack would only propagate in this

region when the crosshead was in motion and that the rate at which load fell off was proportional to the crosshead speed. This behaviour indicates a change from unstable to stable crack growth.

Metallographic examination of the fracture surface

The fracture surface comprised an aggregate of grain surfaces and the topography was very much as would be expected from published photographs of sections normal to the surface. Examination at magnifications up to x150 revealed none of the cleavage step features which typify brittle fractures in body-centred cubic and close-packed hexagonal metals. There was some evidence for dimpling in certain recessed areas but the direct optical technique did have sufficient depth of field for conclusive identification of any features other than those on prominent surfaces in a suitable orientation. All of the areas amenable to optical examination showed smooth surfaces covered in straight slip steps, usually of two orientations. The slip step patterns were much as would be expected where coplanar arrays of dislocations on more than one slip system run out at a free surface. Two typical areas are shown in plates A and B .

Prestrain experiments

The results of the tensile pre-strain experiment, presented in figure 8 indicate that the plastic strain required for fracture during reloading in mercury, decreases as the pre-strain increases and becomes asymptotic to the axis representing zero additional plastic strain. It should be noted however that the fracture stress becomes less than the pre-stress level after about 0.16 strain. This is indicated by the

line labelled '"elastic" fracture line.' During unloading however plastic relaxation occurrs and the reloading curve always deviated from the linear, elastic form below the fracture stress, even at 0.38 pre-strain. It cannot be concluded therefore, as Rosenberg and Cadoff did for brass, that truly elastic brittle behaviour may be induced by pre-strain. On the other hand, although a small amount of deformation always occurred before fracture the results do not prove that this deformation was actually a necessary prerequisite for fracture.

The relative effects of compressive and tensile pre-strain in bending are presented in table 4. Each test sequence is numbered according to the description given in Chapter 3. Comparison of tests 1 and 3 indicates that compressive bending in mercury produces no effect significantly different from that produced by compressive bending in air although there is some evidence that the mercury environment is slightly more damaging. Comparison of tests 1 and 2 indicates that the tensile bending strain in mercury is much more damaging than an equivalent compressive bending strain in mercury or an equivalent tensile bending strain in air. Although test 4 was not performed on the 4.8% bend strain specimens, the results of tests 3 and 4 in the other two batches indicate that tensile pre-strain in air is significantly more damaging than compressive pre-strain. The results are illustrated schematically in figure 9.

The limited investigation of delayed failure indicated that no failure occurrs at constant strain even at strains close to the ductile rupture point. It was noted that the stress relaxed rapidly by plastic flow at all strain levels. In the constant load tests performed on this alloy by Pargeter and Ives (unpublished) therefore, it is impossible to

distinguish between effects due to creep deformation and effects due to stress alone.

Detection of surface damage

Despite considerable scatter, the results of this experiment, presented in table 5 and figures 10 and 11, show that surface damage due specifically to deformation in a mercury environment, exists at a strain which is only 0.7 of the fracture strain or 0.8 of the fracture stress. This damage can be removed by electropolishing and extends approximately to a depth of 3 to 5 microns below the surface.

Examination of the notches in the double notch experiments revealed in most cases a single grain boundary crack at the base of the notch which remained un-fractured. Typical cracks for uniaxial tension and four-point bending are shown in plates D and C respectively. The approximate lengths of these cracks are 40 microns and 30 microns respectively.

Summary:

1. Surface damage to a depth of 5 microns is caused by deformation in mercury well before fracture occurs.
2. Tensile deformation in mercury is necessary to cause this damage although compressive deformation may cause slight damage.
3. After pre-strain in air, some deformation always precedes fracture during subsequent reloading in mercury or during the delay time to fracture at constant load. Delayed failure does not occur at constant strain.
4. Tensile pre-strain reduces the subsequent fracture stress in mercury more than does compressive pre-strain.
5. Crack growth in 1 mm. diameter tensile specimens, indicated by a fall off in load, is very slow initially; the maximum velocity is about 10 mm./sec and appears to be unchanged by a pre-strain of 0.10. Crack velocity slows considerably towards the end of fracture.
6. Cracks in notched bend tests propagate more slowly and the velocity is dependent on the state of pre-strain. A change from unstable to stable crack growth was observed in the later stages of fracture.
7. Extensive plastic deformation occurs in the grains adjacent to the crack and extends to a depth of 0.7 mm.
8. The fracture surface is characterised by smooth grain surfaces covered with slip steps.

CHAPTER V

Discussion

The work described in the two preceding sections has been directed towards an assessment of the role of plastic deformation in the initiation and propagation of cracks due to liquid-metal embrittlement. Questions concerning the role of plastic deformation inevitably arise since this apparently brittle mode of failure occurs in a highly ductile alloy which has been plastically deformed by several percent strain. It would be extremely informative to know whether crack initiation requires plastic deformation or stress alone in the presence of the liquid metal. Once a crack is formed it is equally important to know for all stages of the fracture process whether the crack grows in a stable or unstable manner. For convenience in theoretical analysis or experimental design, it is often assumed that crack initiation and propagation are distinctly separate processes, and that one of them is the critical process determining the susceptibility of the metal to brittle fracture. This distinction has often been made in liquid-metal embrittlement work, though it is quite arbitrary. Westwood (1965) has proposed however that the atomic processes concerned with the interaction of solid and liquid metal atoms are basically the same at both the external surface during crack initiation and at the crack-tip during crack growth. In a similar way, it seems possible that the role of plastic deformation in crack initiation is related to the role of plastic deformation occurring at the crack-tip during propagation. Calculations based on the approach of Kelly et al. (1967) have indicated that if an elastic crack in copper or Cu-17Al alloy is loaded up with mercury at its

tip, then the first process to occur at the crack-tip will be the operation of dislocation sources rather than cleavage. Plastic deformation is therefore expected to occur at the crack-tip; it is important to ascertain whether or not this prediction can be experimentally verified, and to evaluate the role of plastic strain in crack propagation and its relationship to the role of deformation in the initiation process.

The experiments on pre-strain indicate that plastic deformation in mercury under a tensile stress has an effect over and above that due to an identical deformation in air. The curve in figure 8 indicates that if a specimen is pre-strained in air to the level of the fracture strain in mercury then wetted with mercury, fracture will only occur after an additional plastic strain almost equal to the pre-strain. Increasing the pre-strain reduces the additional deformation required for fracture, furnishing strong evidence that a critical applied stress criterion for fracture is not applicable in this case. The effect due specifically to the presence of mercury during plastic straining appears to occur only when the stress is tensile. In the combined bend-tensile experiments the effect of wetting the side which undergoes compression in bending (test 1) gives rise to fracture stresses and strains which are not significantly different from those in test 3 where mercury was applied to the same side but after straightening. Comparison of tests 3 and 4 indicates that tensile pre-strain in air reduces the subsequent fracture stress in mercury more than does compressive pre-strain in air, but this effect cannot account for all of the difference between compressive and tensile deformation in mercury.

Further evidence for effects due specifically to mercury during

plastic deformation, is furnished by the intermediate electropolishing experiments. Electropolishing restored the condition of the wires from that corresponding to deformation in mercury to that corresponding to a similar deformation in air. i.e. the effects due specifically to the presence of mercury were removed. This experiment indicates not only that the effect of the mercury is already detectable at 0.8 of the fracture stress but also that the effect is localised within about 5 microns of the surface.

Since the additional deformation required in mercury after pre-strain in air decreases as the amount of pre-strain increases, the possibility arises that at some high pre-strain no further deformation will be required in mercury and fracture will occur after purely elastic loading. The curve relating strain in mercury to pre-strain (figure 8), however becomes asymptotic to the y axis and even at pre-strains close to the ductile rupture point a small amount of plastic strain precedes fracture. The plastic relaxation which occurs in this metal when straining is halted will always give rise to some plastic strain prior to fracture. An experiment using very high pre-strains obtained in compression suggests itself but the difference in the effects of compressive and tensile pre-strains already noted above will lead to ambiguous results.

One important feature to be noted in the pre-strain curve of figure 8, is that there is no discontinuity in the slope of the curve where fracture occurs at the pre-stress level. This point is marked by the line labelled, ' "elastic" fracture line'. At higher pre-strains, the plastic strain preceding fracture is within the level of plastic relaxation which occurs on unloading from the pre-stress level. Rosenberg

and Cadoff (1963) have plotted fracture stress versus pre-strain for α-brass embrittled by mercury and obtained a maximum stress where fracture occurred at the pre-stress level. If plastic relaxation occurred on unloading however the fractures occurring at higher pre-strains cannot be described as 'elastic' brittle fractures.

The occurrence of slight plastic deformation prior to fracture at high pre-strains does not necessarily show that such deformation is an essential prerequisite to fracture. Some indirect evidence that the deformation is necessary can be deduced from the delayed failure characteristics. Cu-17Al alloy undergoes considerable plastic relaxation when straining ceases. In constant strain this gives rise to a rapid fall off in stress; in constant load extensive creep deformation occurs. Delayed failure in mercury is only observed under constant load conditions indicating a need for plastic deformation. Since it is impossible in this system to observe the effects of stress without plastic deformation occurring, any attempt to distinquish between effects due to deformation and effects due to stress alone will be ambiguous. It is informative therefore to compare the results for Cu-Al alloys with those for age hardenable alloys in which plastic relaxation is much less likely to occur. Age hardened Cu-2%Be and 2024 aluminum alloys have both been observed to fail in mercury at constant strain and furthermore, Nichols and Rostoker (1965) succeeded in showing that when Cu-2%Be was held in mercury at constant load, no micro-creep occurred prior to fracture. These observations indicate that it is possible for liquid-metal embrittlement to occur without plastic deformation in the micro-creep range taking place in the presence of the liquid metal. It is still possible however that highly localised dislo-

cation activity is sufficient to initiate fracture in these high strength alloys.

The results of the micro-hardness and x-ray diffraction experiments show quite conclusively that extensive plastic deformation has accompanied fracture. In Chapter 2 the possibility was discussed that plastic deformation at the crack-tip might be due to the inability of the liquid metal to keep up with the propagating crack. In this case the deformation observed would not give very much information about the crack propagation process. If on the other hand, plastic deformation occurs even in the presence of liquid metal, then a measurement of the extent of deformation could be extremely valuable. Several observations indicate that liquid metal supply rate is not the factor controlling plastic deformation. The wire specimens were only 3 mm. diameter and care was taken to ensure that a plentiful supply of mercury was available. The maximum distance of the crack from the mercury supply at the surface was only 1.5 mm. whereas the crack velocity measurements quoted by Rostoker (1960) refer to measurements in the crack length range of 0.5 to 6 inches. In a case where cracks propagated through brass sheet only 0.020 in. thick with mercury along the entire crack path, Rostoker's visual measurements of instantaneous crack length indicate a velocity of only 6 in./sec. There is evidence therefore that even with an adequate mercury supply system the crack velocity in brass is much lower than in age hardened aluminum alloys in which crack velocities of up to 300 in./sec. have been measured. Rostoker has proposed that the factors controlling the supply of liquid metal to the crack tip are the distance of the meniscus from the tip and the rate of surface diffusion of liquid metal atoms on a monolayer of the same species. Since

a rate of 300 in./sec. is attainable in 2024-T4 aluminum alloy there is no doubt that when an adequate supply of liquid metal is available it will always be present at the crack-tip in brass where the crack propagates at a rate which is two orders of magnitude lower. Copper-aluminum alloys should display crack velocity characteristics similar to brass. In order to check the effect of mercury supply as well as possible a 1 mm. diameter wire was fractured in an adequate mercury supply and micro-hardness readings taken as with the 3 mm. diameter specimen. The results are given as Z_{11} in figure 1 and are similar to those for the 3 mm. diameter specimen in spite of a larger grain size. As well as can be ascertained therefore there is no effect of mercury supply rate on the crack velocity and on the plastic deformation at the crack-tip. Estimated crack velocities from figure 7 are of the order of 1 cm./sec. and therefore correspond with the order of magnitude observed for brass.

The distribution of plastic strain at the fracture face is similar in both micro-hardness and x-ray diffraction estimates. At distances greater than 0.1 mm. from the surface however the strains indicated by the x-ray results are higher than those for the micro-hardness studies. The reason for this is difficult to ascertain. Since only three specimens have been given a complete examination it is possible that real variations in plastic deformation are being recorded. Spurious effects such as surface topography may however, affect the x-ray diffraction line broadening in some way. An annealed fracture surface was found to give the same line width as a plane surface but the effects of a deformed surface cannot be checked in this way. The variations between the three curves of figure 1 give rise to an order of magnitude difference in the energy of plastic

deformation but the maximum strains at the fracture surface are similar.

The estimated shear flow stress at the crack tip is given in table 3. Values in the range 2.5 to 3.5 x 10^9 dynes/cm^2 are calculated. These values are less by at least a factor 3 than the minimum value required by the theory of Kelly et al. (1967) for cleavage to occur at the crack-tip before dislocation sources are operated by the concentrated shear stresses. If however, the theoretical estimate of cohesive strength, due to Orowan (1949) is an overestimate by a factor of 2 as Kelly (1966) has indicated for diamond and sodium chloride crystals then:

$$\frac{\sigma_{max}}{\tau_e} \simeq R \text{ (plane strain)}$$

where τ_e is the estimated flow stress at the crack tip. The possibility of cleavage therefore arises if the grains ahead of the crack are work hardened to a shear flow stress of τ_e by the strain concentrating action of the crack.

From the foregoing discussion of results it is apparent that a theory of liquid-metal embrittlement cannot be based upon a critical applied stress criterion for fracture nor can it assume that the critical process is the initiation step since this implies that once a crack has formed the conditions necessary for propagation are already fulfilled by the level of applied stress and uniform strain. A theory of liquid-metal embrittlement must be able to account for the following:

1. The cumulative effect of tensile deformation in an embrittling liquid-metal environment which causes surface damage over a period of increasing applied stress starting well before fracture,

2. The nature of this damage and the significance of the applied stress at which the load drop starts to occur,
3. The relationship between stress, time and plastic deformation with particular reference to the effects of pre-straining and age-hardening,
4. The mechanism of crack propagation and the effect of the large amount of plastic deformation observed to accompany crack propagation.

The critical pile-up length model based on the work of Petch (1953) and Stroh (1957) has been used frequently to describe the liquid-metal embrittlement phenomenon and it is of interest to compare the assumptions and characteristics of the theory to the four points outlined above. The pile-up model is essentially a critical stress theory for fracture which predicts that crack initiation is the critical process. Stroh's analysis indicates that the crack formed is unstable and propagates to fracture unless halted by an obstacle. Although the initiation process is a microscopic one involving a particular dislocation pile-up, the theory has been developed in terms of measurable macroscopic parameters such as applied stress and grain size, and a critical applied stress for fracture is predicted. Grain size and stacking fault energy variations give qualitative support for the applicability of this theory to liquid-metal embrittlement. In particular, the straight line obtained by plotting fracture stress against square root of grain size has been taken as confirmation of the validity of the approach. The slope of the line gives a value of the surface energy which is appropriate to micro-crack formation and which contains a plastic work term. Values obtained for surface energy are at least three orders of magnitude less than the value of 10^8 ergs/cm^2

measured in this work for crack propagation. Furthermore the use of slopes to calculate surface energy can give rise to anomalous results. In the work of Pargeter and Ives (1967) for instance the slopes of the lines indicate that the effective surface energy in Cu-Al alloys increase with the aluminum content. If however individual fracture stresses for the same grain size in different alloys are fed into the formula relating fracture stress and grain size, then the predicted surface energies vary in the opposite sense with increasing aluminum content. The slopes of the lines obtained by Pargeter and Ives (1967) are close to the slopes obtained for yield stress versus square root of grain size, and vary with alloy content in the same way as yield stress slopes. It seems doubtful therefore that the slopes of these lines have anything to do with a critical fracture stress or surface energy. In a similar analysis of the grain size versus fracture stress data of Rosenberg and Cadoff (1963) it was found quite impossible to extract any sort of critical fracture stress criterion.

Since the pile-up theory contains no parameters which are time dependent, the theory cannot explain delayed failure and since it is based on a single critical initiation event it cannot explain the cumulative damage observed to occur during tensile plastic deformation in the liquid-metal environment. It seems evident however that grain size and stacking fault energy do play some part in the fracture process. The weakness of the pile up theory in its application to liquid-metal embrittlement, is that it attempts to describe fracture in macroscopic terms. It would seem more informative to consider the effect of dislocation pile ups in microscopic terms without making assumptions about the relative difficulties in initiating and propagating cracks.

The evidence relating to the effects of compressive and tensile plastic deformation in mercury indicates quite strongly that the cumulative surface damage produced is in the form of small grain boundary cracks or incipient cracks along which mercury has penetrated under the action of tensile deformation. This interpretation is strengthened by the observation in this work, that cracks are present just before fracture, and in the work of Levine and Cadoff (1964) that cracks exist at a stress which is only 0.8 of the fracture stress. The period of increasing applied stress over which these cracks form and grow may then be regarded as a period of crack initiation and stable crack growth, and the observed fracture stress is not a critical initiation stress but the stress at which a crack has grown long enough to become unstable. The condition for instability will depend upon the mode of propagation; although grain size and stacking fault energy may be influential in determining the conditions for instability they will no longer act through a critical stress criterion. Prediction of the fracture stress is not therefore a question of the critical initiation event but an estimation of several equally important effects:

1. What is the effect of the metallurgical conditions and mechanical properties on the rate of growth of a stable crack?
2. What factors determine the critical conditions for the transition from stable to unstable crack growth?

The answers to these questions require a knowledge of the mechanism of crack propagation in both stable and unstable modes. Growth in an unstable manner has been examined more directly in this work than the initial stages but the two stages of fracture are probably related. Although the critical applied stress theory has not proved to be valid,

the idea of a critical local stress is still an intuitively plausible basis for the embrittlement phenomenon. Rather than a single critical event however, a whole series of similar critical events may be envisaged giving rise to crack growth. The calculations based on the theory of Kelly et al. (1967) have assumed that fracture will occur if the theoretical cohesive stress is reached. This normal stress can only be attained if the critical stress for shear processes can be raised, in the region of the crack tip, to a value greater than the concentrated shear stress at the crack-tip. Estimates of the plastic strain at the crack-tip indicate that the strain concentrating action of the crack may work harden the grains adjacent to the crack path sufficiently to raise the local flow stress above the critical level. Plastic deformation at the crack tip, however, will give rise to dislocation pile-ups some of which will be driven up against the grain boundary right at the crack-tip as in Figure 12. Slip will relieve the overall stress concentration and the total energy change due to plastic deformation at the crack-tip must be negative, according to the law of thermodynamics. The pile-ups running up against the crack tip may create over small volumes however, even greater stress concentrations than that due to the crack. The relevant quantities to consider, therefore, may be the normal and shear stresses at the head of these dislocation pile-ups rather than those due to the crack itself.

It is important to recognize that whichever of these two stress concentrating processes gives rise to crack growth, the area susceptible to brittle fracture is at all times restricted to the immediate vicinity of the crack tip. At any instant during fracture, the area ahead of the

crack in an embrittled condition is limited to that region in which cohesive strength is reduced by the presence of liquid metal atoms and throughout which the normal stress is at least as high as the reduced cohesive stress. If there is a well-defined crack tip and no penetration of liquid metal beyond the tip, then only the bonds between those atoms bounding the tip can be weakened at any instant. The concentration gradient of liquid metal atoms over the first few atomic spacings ahead of the crack will however, be very great and it seems likely, especially in view of the disordered nature of the grain boundary that liquid metal atoms will be able to penetrate ahead of the tip. The penetration time over the first few atomic spacings will be of the order of the period of atomic vibrations, far smaller than the observed time for crack growth and so an area of weakened grain boundary will always precede the crack-tip.

Since the deformation accompanying fracture has been observed to extend over about ten grains adjacent to the crack, it seems likely that extensive work hardening is necessary to raise the flow stress no matter what the origin of the normal stress concentration that gives rise to fracture. Plastic deformation at the crack tip is an essential prerequisite to fracture and probably plays a two fold role in the fracture process: first the deformation raises the internal stress by work hardening and second, the deformation creates a pile-up of dislocations at the crack tip in the high internal stress field; this internal stress prevents relaxation of stress by shear processes and enables the pile-up to grow to sufficient size to cause an increment of crack growth. This raising of the internal stress and pile-up formation must occur continuously at the crack tip throughout crack propagation. It is emphasized once more

that at the onset of fracture, the only material whose mechanical condition may be described as brittle is that small volume at the crack-tip which is in contact with the liquid-metal atoms and which has been sufficiently work-hardened that there can exist in it, a concentrated normal stress equal to the reduced cohesive strength. The remainder of the metal cannot be described as intrinsically brittle under the prevailing conditions of uniform plastic strain and applied stress. This includes both the grain boundaries ahead of the small penetrated region at the crack tip which eventually form the crack path, and the external surface layer which has been deformed in contact with the liquid metal.

Both compressive and tensile forces can give rise to the required internal stress level and create the brittle region at the crack tip. However, only a tensile force can cause total fracture since the embrittlement of the next increment of grain boundary requires the crack tip to extend into the brittle area causing further plastic deformation ahead of itself. Only a tensile force can open up and extend the crack in this way. This can explain not only why total fracture cannot occur in compression but also why, in the bend-tensile tests, compressive and tensile deformation of mercury coated wires prior to fracture had different effects on the subsequent behaviour of the wires when deformed and fractured in uniaxial tension. In the wires where tensile bending occurred in the presence of mercury, any cracks formed before total fracture would be able to grow whereas cracks on the compressive side would not. The different effects of compressive and tensile pre-strain in air are less easy to explain. The internal stress level will for a given strain be independent of the sign of the strain. Since the experiment

imposed a final, uniaxial tensile strain on to a compressive, bend pre-strain a Bauschinger effect may be the source of the observed differences. For a given uniaxial tensile strain, the dislocation densities will be similar for compressive and tensile pre-strains but the reversal of stress in the former may result in lower internal stress concentrations since un-pinned pile-ups at grain boundaries will tend to run back towards their source.

Although the estimates of the energy of plastic deformation per unit area of fracture surface vary by a factor 3, the order of magnitude is undoubtedly 10^9 ergs/cm^2 which is higher by four orders of magnitude than the largest values obtained by Petch-Stroh model calculations. It is important to note that in the fracture models proposed above, whether the fracture is the result of stress concentrations due to the crack or to the pile-ups at the crack tip, the overwhelming amount of plastic deformation contributing to this high energy value occurs ahead of the crack and not right at the crack-tip during the actual parting of atomic bonds. Thermodynamically, it is still correct to add plastic deformation energy and surface energy in describing the criterion for unstable crack propagation. However, once the plastic deformation has raised the internal stress level ahead of the crack to the necessary level, the important quantity controlling fracture is the true surface energy since it is this quantity which controls the cohesive strength of the grain boundary and the stress level required to part the atomic bonds across it.

The slip steps observed on the fracture surface have not hitherto been discussed. It is possible that a more detailed examination of the step spacing and height can give an estimate of the plastic strain accompanying fracture and possibly some information on the role of pile-ups

in the fracture process. Beyond the simple observation that the steps are very coarse and very long and straight, there is little that can at present be said however, about the significance of the fractographic study. A possible mechanism for the formation of the steps is illustrated in Figure 12.

The fracture mechanism proposed has been developed for the stage at which a crack propagates in an unstable manner causing a rapid decrease in the observed load. If a period of stable crack growth is postulated to occur prior to the onset of observable unstable propagation, then a stable growth mechanism is also required. It seems reasonable to assume that the initial stages of fracture have some basic similarities to the final unstable crack propagation, in particular with reference to the role of plastic deformation in continued growth and the requirement that the cohesive stress is reached locally. If there is a period of stable crack growth then propagation could occur by the same strain concentrating mechanism that operates during unstable growth, requiring plastic deformation to occur continuously at the crack tip. In this case, however, the strain concentrating action would be small due to the short length of the crack and growth could continue only by raising the applied stress. The transition from stable to unstable growth must then be concerned with the degree of strain concentration at the crack-tip. The transition to unstable growth occurs when the crack has grown sufficiently long that the plastic deformation at the crack-tip necessary for crack growth can occur without further increase in the applied stress. At this point, the strain concentrating action of the crack is sufficiently large to cause the plastic deformation necessary for fracture by utilising only the

elastic energy stored in the stress system. If the elastic energy supply runs out before fracture is complete then crack growth will halt or proceed only at the rate that energy is supplied by an externally applied strain rate. This is probably what was observed in the notched bend tests in Figure 7. The reduced crack velocity at the end of fracture in the uniaxial tensile tests is more complex to interpret however due to the oscillations in load in this region.

Although no estimates have been made of the plastic deformation accompanying fracture in a pre-strained specimen, the theory outlined above indicates that less additional deformation would be required to reach the required stress level at the crack-tip. If crack velocity is controlled by the quantity of deformation necessary at the crack-tip, then a higher velocity may be expected in a pre-strained specimen. For the pre-strained bend specimen in Figure 7 this is indeed observed but not in the pre-strained tensile specimen. The larger total amount of elastic energy available in the latter may account for the independence of velocity.

It would also be expected that metallurgical condition and intrinsic strength would influence crack velocity since in a high strength material a small amount of deformation would be necessary to raise the local flow stress at the crack-tip to the critical level. This prediction is in accord with the observed difference in crack velocities between 2024-T4 aluminum alloy and annealed brass. (Rostoker, 1960). Intrinsic strength would also reduce the amount of stable crack growth required to reach the critical length for instability since the smaller strain concentration needed would require a proportionately shorter crack length. This would account for the observed effects of pre-strain and greater susceptibility

of higher strength metals to premature failure in an embrittling liquid metal environment.

The problem of crack initiation remains even if stable crack growth accounts for almost all of the period of increasing applied stress over which damage occurs. No experimental evidence has been obtained in this work to justify the postulation of any specific mechanism. However, two general remarks can be made. Firstly, if stable crack growth precedes fracture, then the initiation event is not critical since it does not lead directly and immediately to total fracture. Only where the flow stress is raised to such a level that only a very small amount of stable growth occurs, is the initiation event critical. Secondly, it seems reasonable to postulate that since stable crack growth requiring an increasing applied stress is not possible in cases of delayed failure at constant load or constant strain, then the initiation mechanism must be able to cause continued growth of a crack or incipient crack to the critical size required for instability. The mechanism will be time and stress dependent suggesting some thermally activated process.

One piece of evidence which must be taken into account is that delayed failure at constant strain only occurs in metals or alloys where the dislocation arrays do not relax significantly when straining ceases. This suggests that stress concentrations at the head of pile-ups must be maintained for the growth of a crack or incipient crack to the length at which unstable propagation becomes possible.

A number of mechanisms may possibly be involved including grain boundary grooving, stress enhanced grain boundary diffusion and stable micro-cavity formation at the head of pile-ups. Experimental evidence

relating to the stages of embrittlement prior to fracture is however very sketchy and it is quite possible that the initiation mechanism and stable growth mechanism are essentially the same.

Conclusions

Experimental results have been summarized in Chapter IV. Since the significance of all the results is not immediately obvious, the interpretations are re-iterated below.

1. During fracture, the crack propagates slowly and is accompanied by extensive plastic deformation. It seems improbable that the mechanics of supplying mercury to the crack tip control the crack velocity and it is concluded therefore, that plastic deformation at the crack tip is an integral part of the fracture process.

2. Evidence relating to the effects of deformation in mercury prior to fracture provides strong indication that a period of stable crack growth precedes fracture.

3. Experimental work on pre-strain effects and analysis of data relating to effects of grain size, yield stress and stacking fault energy all indicate that a critical applied stress criterion for fracture is not applicable.

A model for liquid metal embrittlement has been proposed to describe the processes occurring after initiation of a stable crack.

a. The criterion for incremental extension of the crack, whether stable or unstable, is that the normal stress concentration over this increment ahead of the crack tip be equal to the cohesive strength of the grain boundary in this region.

b. At any instant during fracture, the only region which can be

described as brittle is this small area of grain boundary ahead of the crack tip over which the normal stress is greater than the critical value and into which the liquid metal has penetrated.

c. In order for the normal stress to reach the cohesive strength, the shear flow stress must in general be increased by plastic deformation and work hardening. The extent of plastic deformation required will depend upon the intial flow stress prior to application of liquid metal, and the rate of work hardening.

d. If the applied stress for plastic flow prior to wetting with liquid metal, is less than the cohesive strength then further plastic deformation must occur in the presence of the liquid metal. After a crack has been initiated then this deformation may occur locally at the crack-tip since the crack acts as a strain concentrater. Crack growth can only be as fast as the rate of plastic deformation at the crack-tip.

e. Unstable crack growth can occur only when the strain concentrating action of the crack can cause sufficient plastic deformation for crack growth without an increase in applied stress. Stored elastic energy in the stressed system is then sufficient to maintain propagation. If crack growth occurs prior to this then the crack must be stable requiring an increasing applied stress for growth.

f. The amount of stable crack growth will be related to the amount of plastic deformation required for fracture in excess of the uniform plastic strain. It will, therefore, be related to the flow stress prior to wetting with liquid metal.

g. The local stress concentrationwhich causes an increment of growth at the crack-tip may be regarded as being due to the crack itself or to

pile-ups at the crack-tip created by the strain concentrating effect of the crack. Since the crack is not an elastic type of crack, the latter seems to be the most realistic view point.

h. A crack initiation mechanism is required which gives rise at first to a stable crack and which can also give rise over a period of time at constant load to an unstable crack. Some possible mechanisms have been enumerated but there is no experimental justification for any further speculation in this area.

Suggestions for Future Work

The fracture model proposed herein predicts certain effects which should be experimentally verifiable.

1. By metallography and surface replication, it should be possible to establish the strain at which cracks form, the depth of the cracks and rate of growth if such cracks do in fact grow in a stable manner.

2. By double notch experiments it should be possible to establish the crack length at which unstable propagation commences. A variation of this length with such parameters as grain size pre-strain, solute content and metallurgical condition seems probable according to the model.

3. Some calculations on the strain concentrating effect of cracks would be useful in conjunction with the above.

4. Using either x-ray diffraction line-broadening or micro-hardness it should be possible to verify the predictions of the model concerning variations of the plastic deformation accompanying fracture with pre-strain solute content, grain size and metallurgical condition.

5. Crack velocity variations with the same parameters as above would also be informative but the experiments must be carefully designed to

ensure that the parameter being varied is indeed the controlling factor. Problems concerned with liquid metal supply must also be eliminated.

6. The identification of an initiation process distinct from the stable growth phase is difficult and must await further information on the early stages of crack growth. Delayed failure experiments may be the most profitable in studying the initiation stage.

Fig. 1

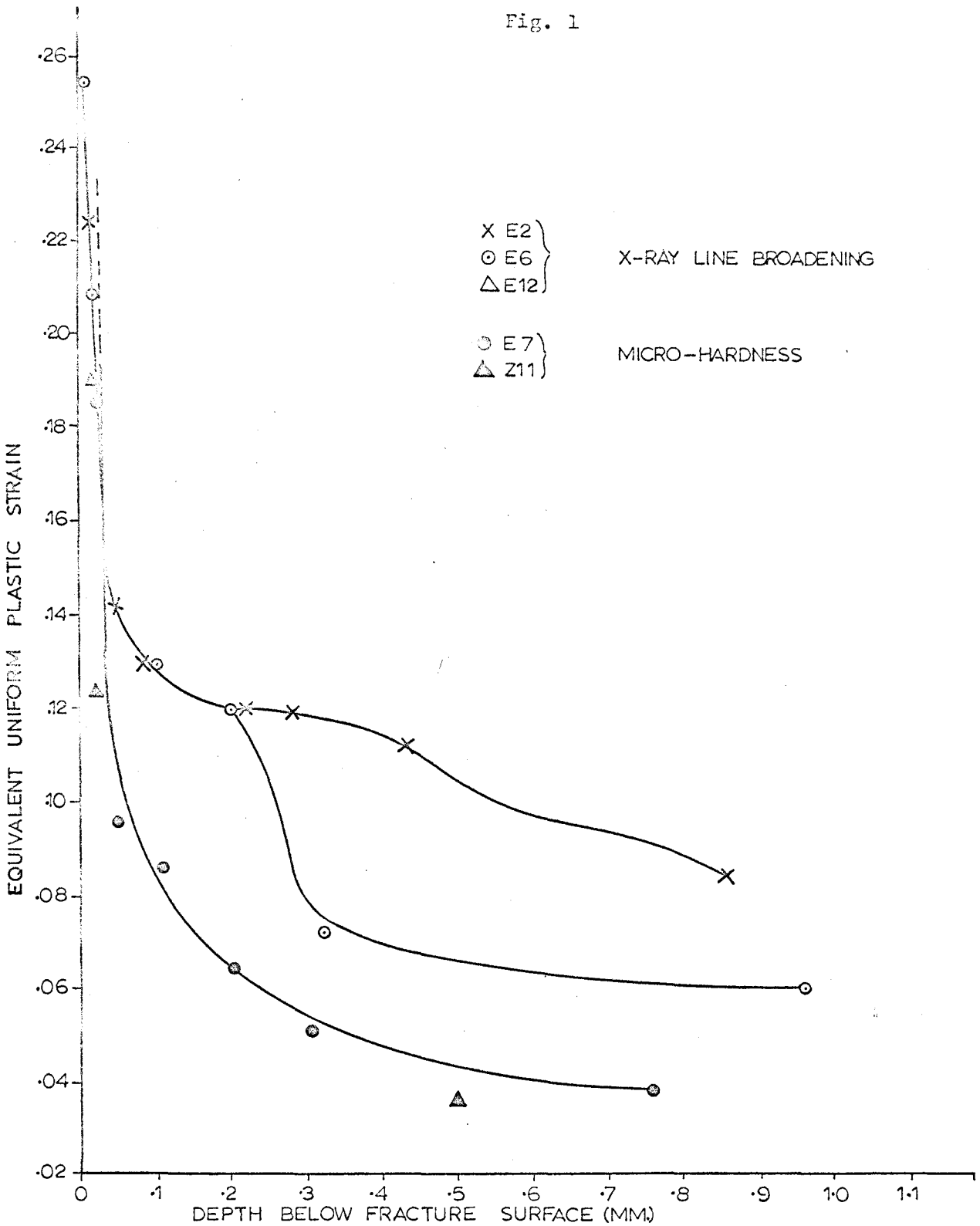

Fig. 1, PLASTIC STRAIN AT THE FRACTURE SURFACE

Fig. 2

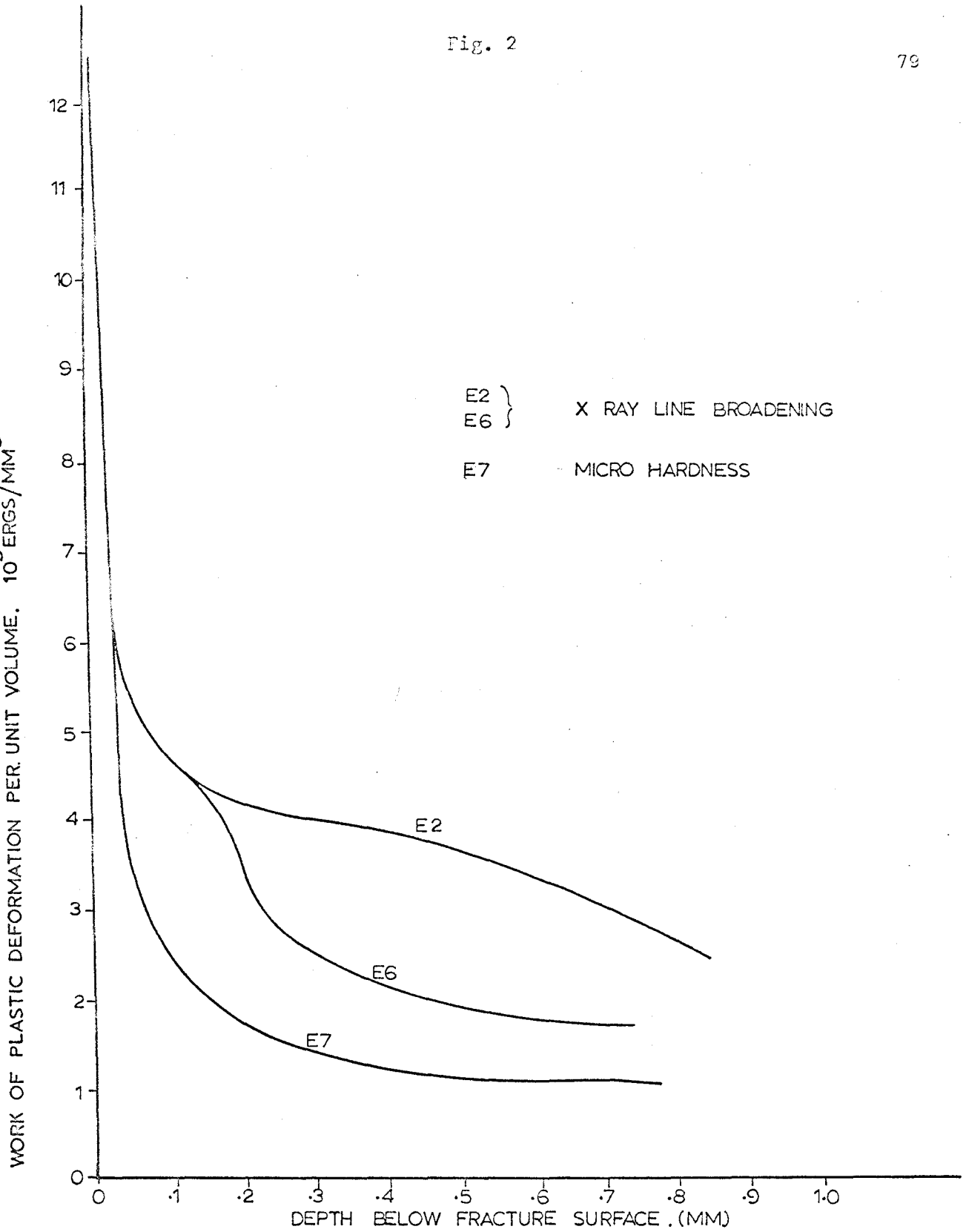

Fig. 2, WORK OF PLASTIC DEFORMATION AT THE FRACTURE SURFACE

Fig. 3

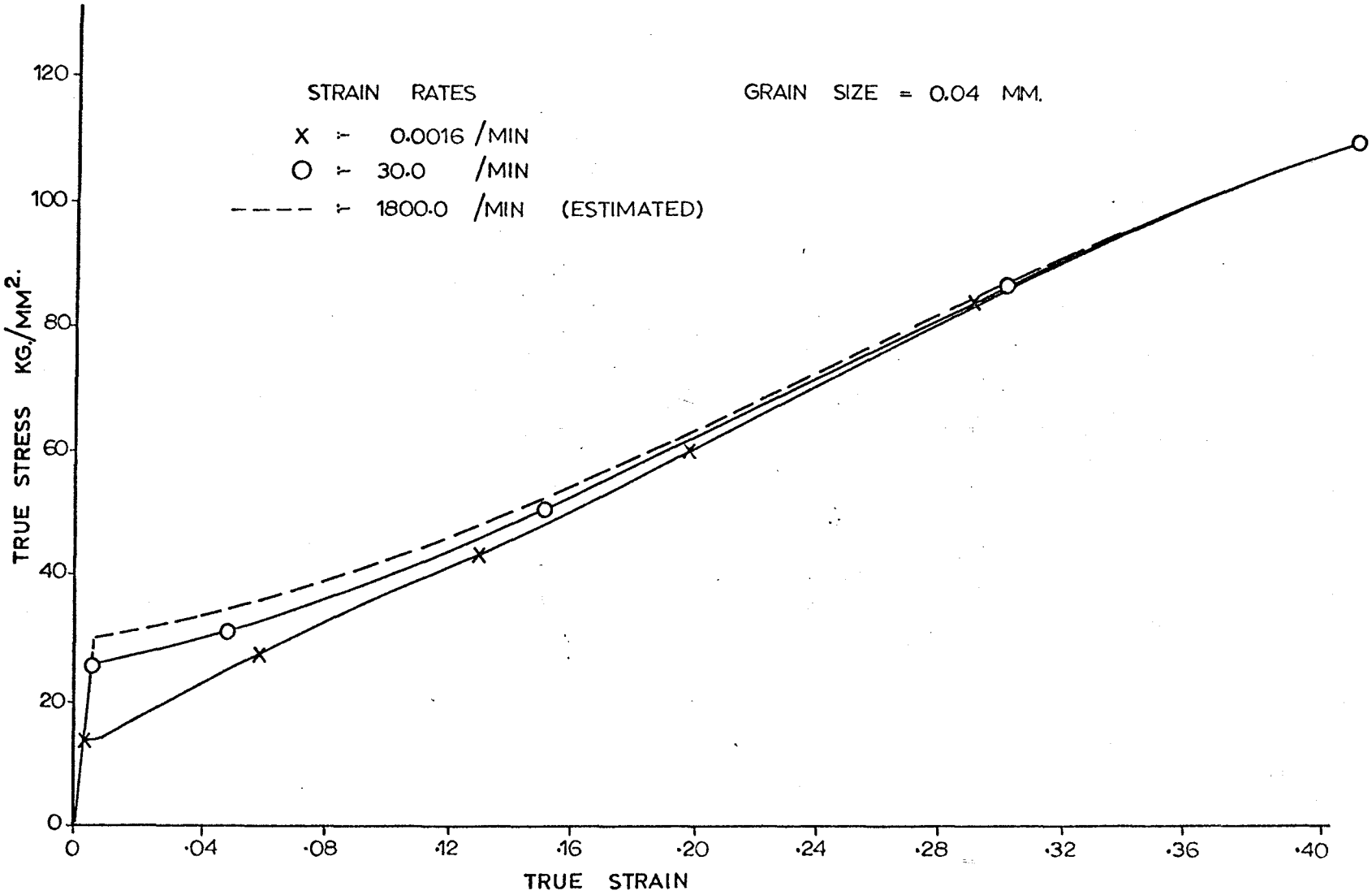

Fig. 3, STRESS STRAIN CURVES FOR Cu-17Al. AT WIDELY DIFFERENT STRAIN RATES

Fig. 4

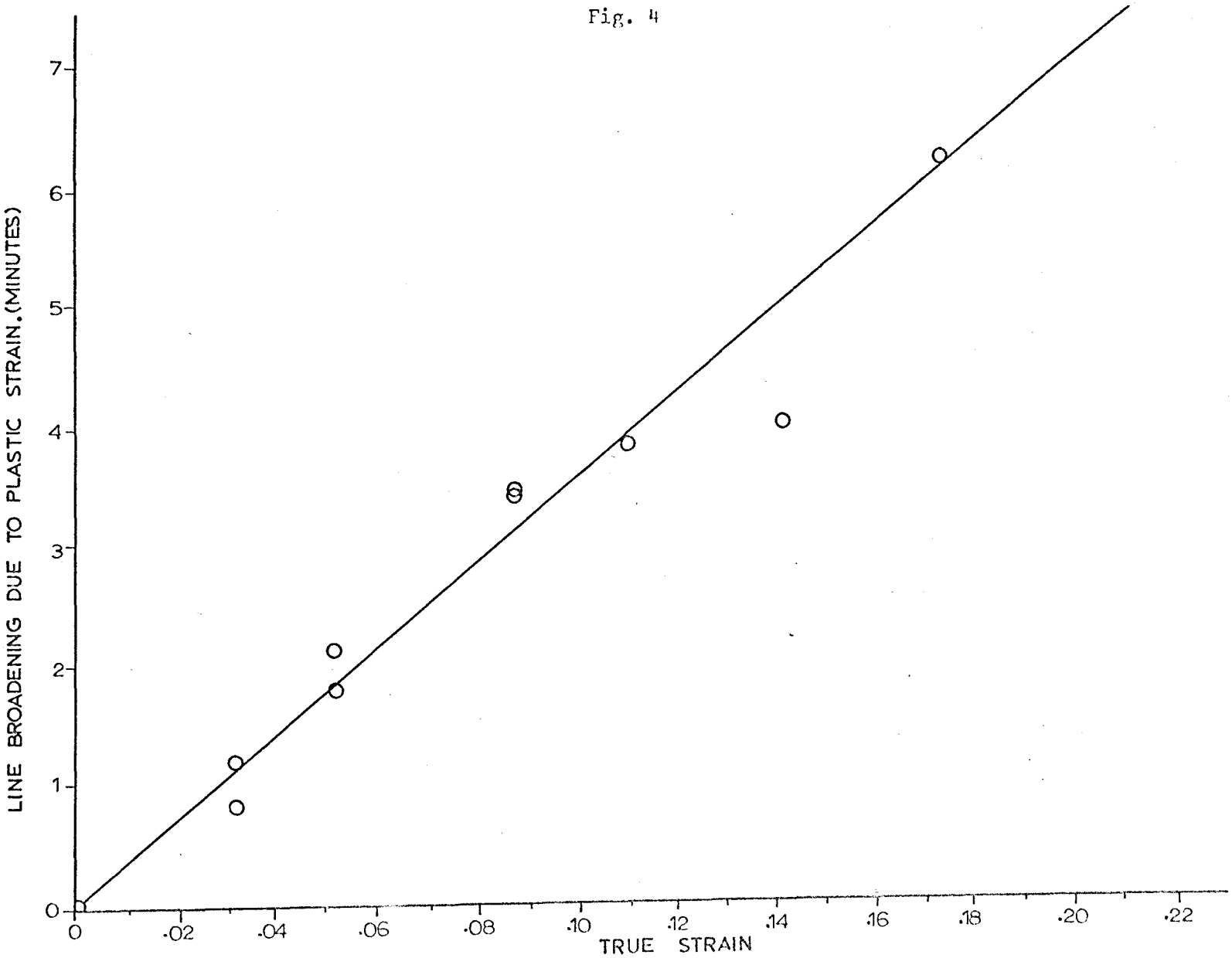

Fig. 4, X-RAY LINE BROADENING VERSUS PLASTIC STRAIN FOR C_U-17 Al STANDARDS

Fig. 5

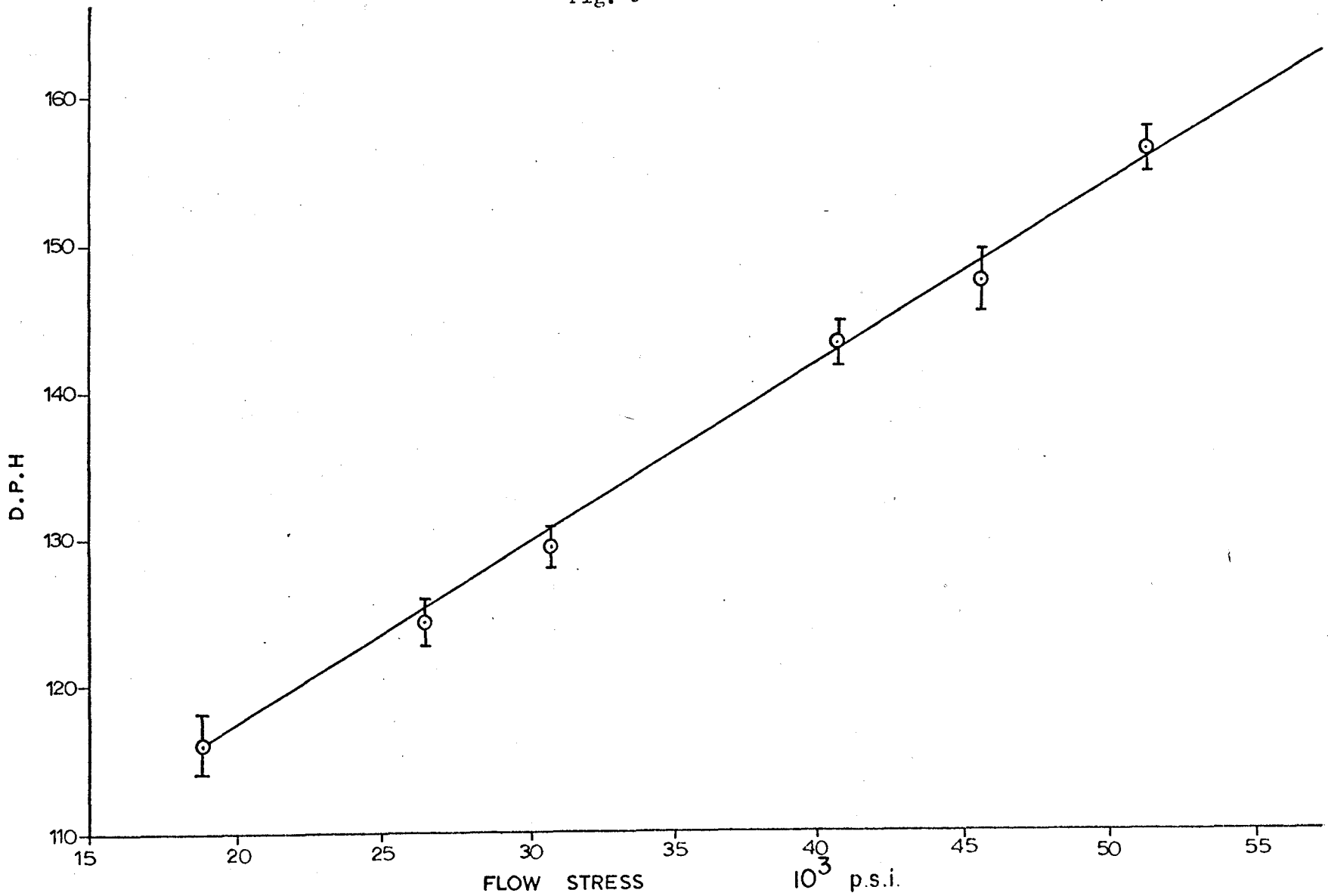

Fig. 5, Micro Hardness Versus Flow Stress for C_u17Aℓ Standards

Fig. 6

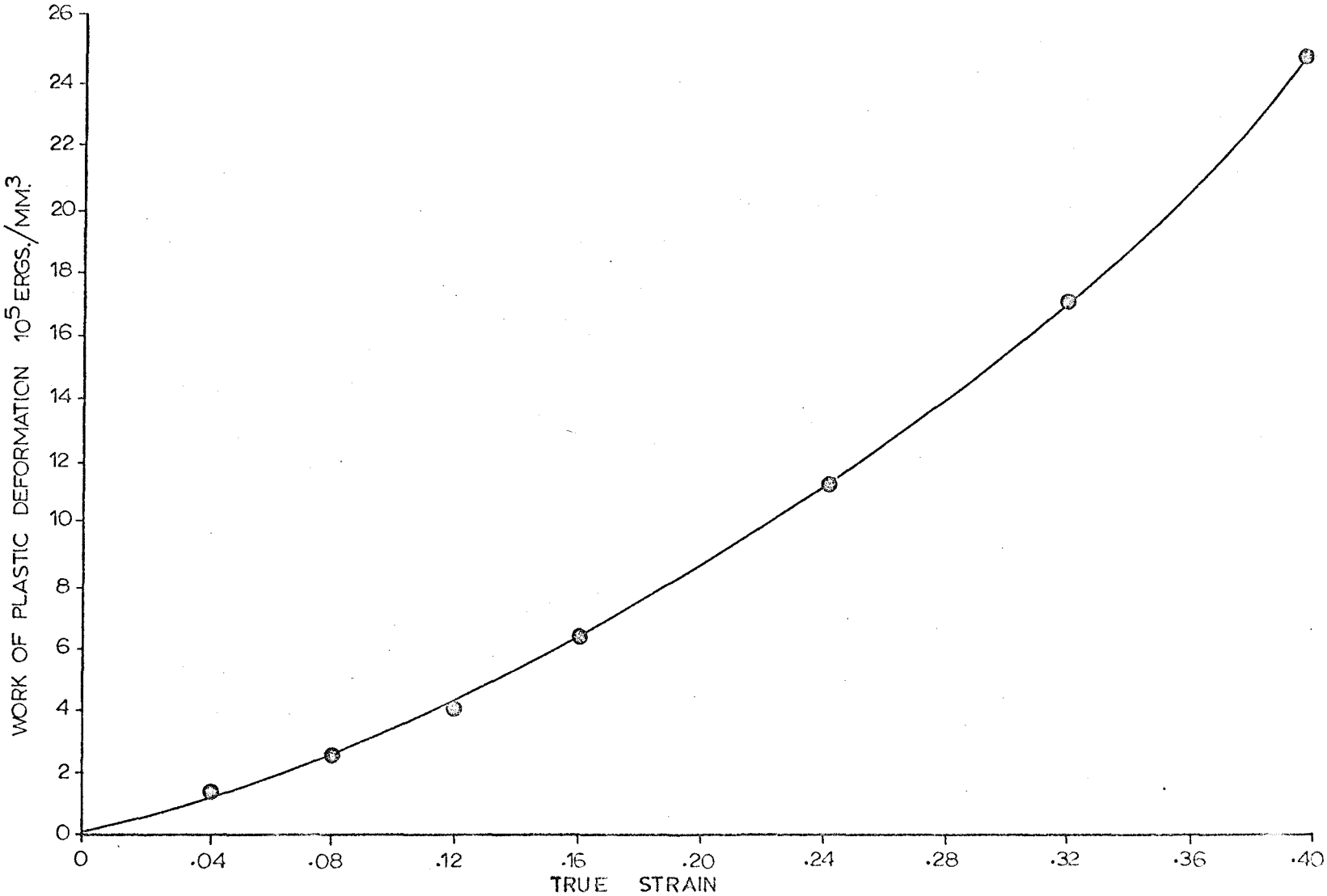

Fig. 6, WORK OF PLASTIC DEFORMATION VERSUS STRAIN, FOR A STRAIN RATE OF 1800.0 PER MIN

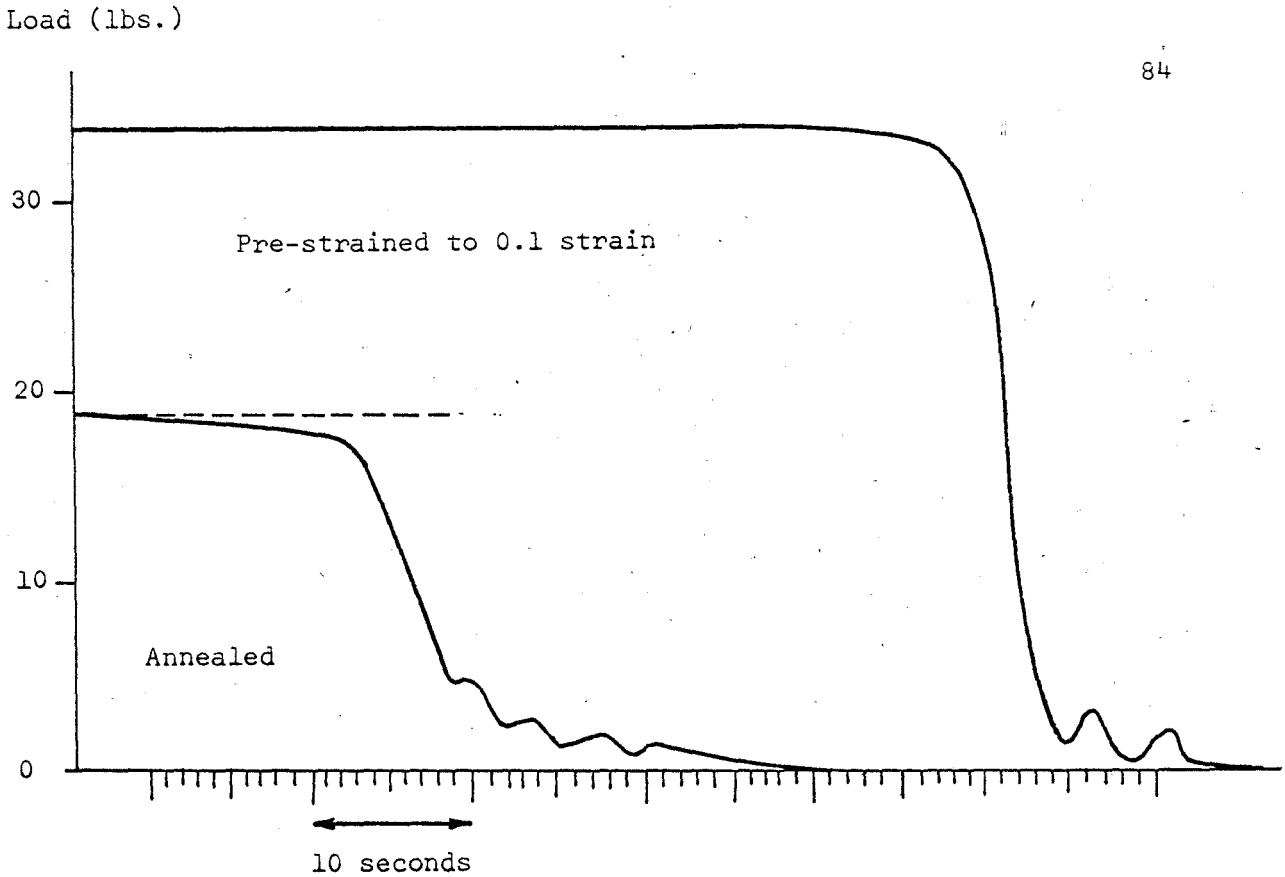

Fig. 7a. Uniaxial Tension

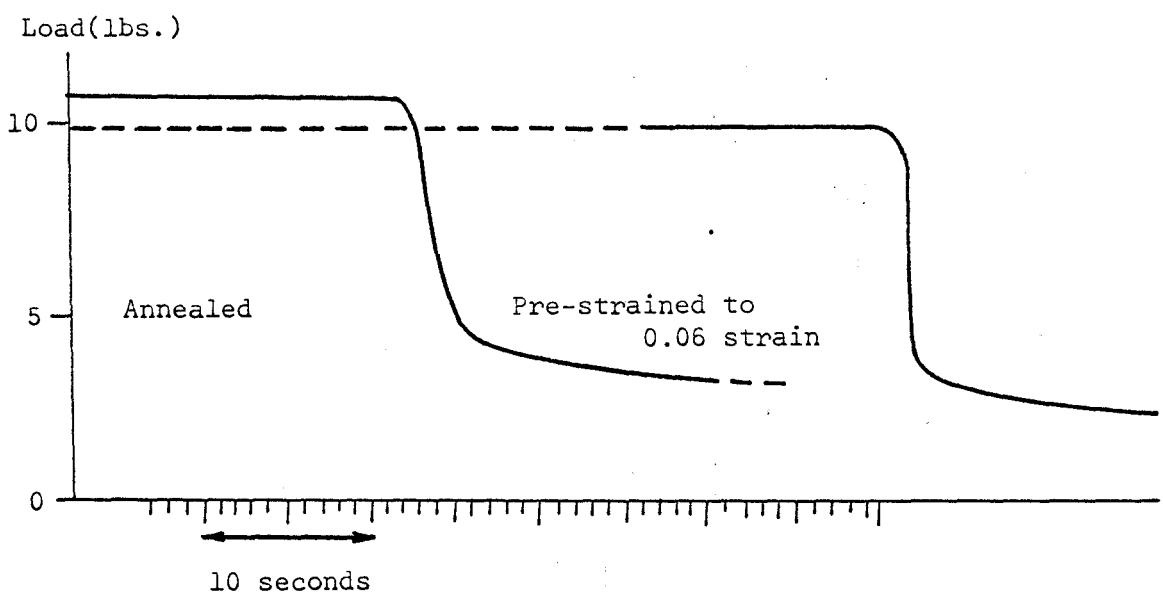

Fig. 7b. Four Point Bending

Fig. 7, LOAD VERSUS TIME AT FRACTURE

Fig. 8

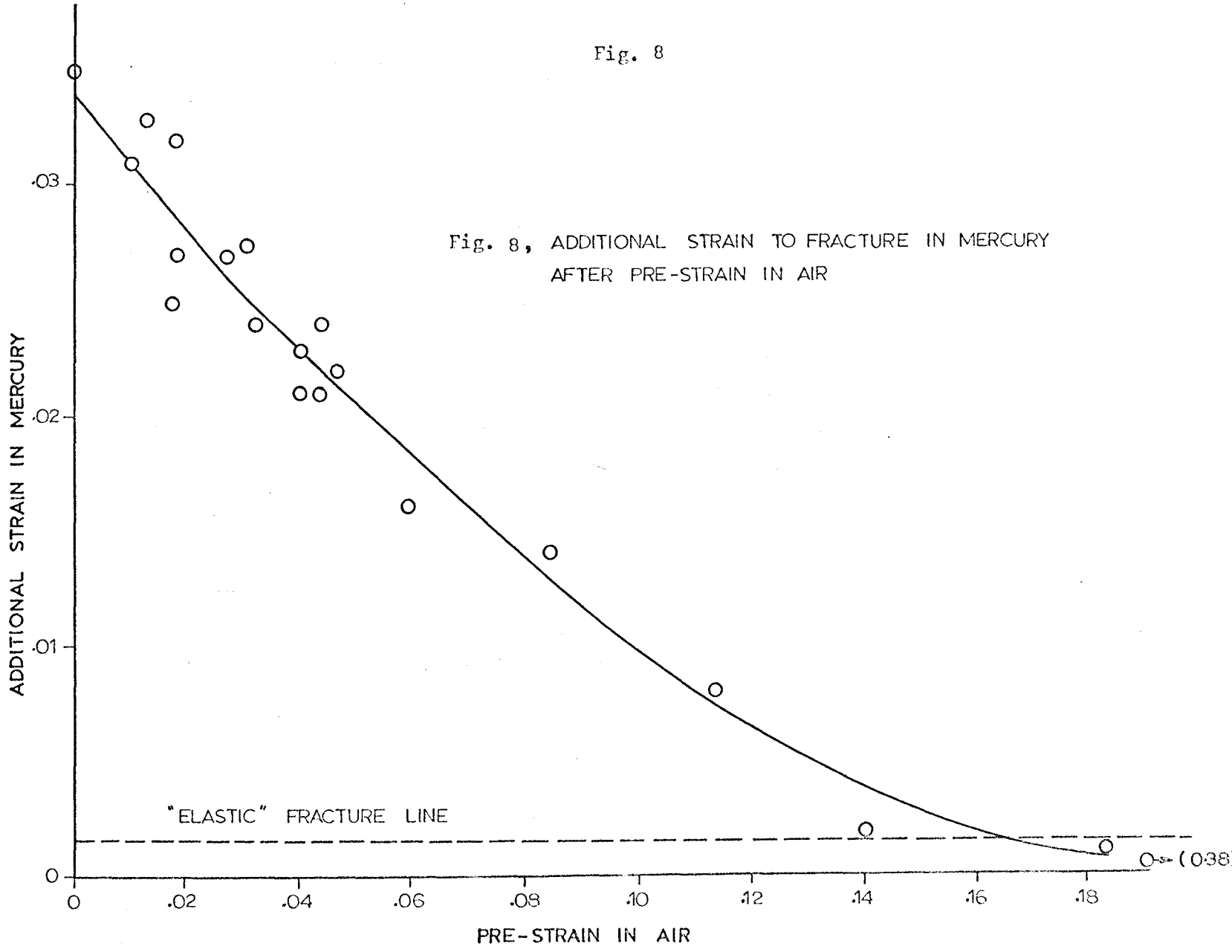

Fig. 8, ADDITIONAL STRAIN TO FRACTURE IN MERCURY AFTER PRE-STRAIN IN AIR

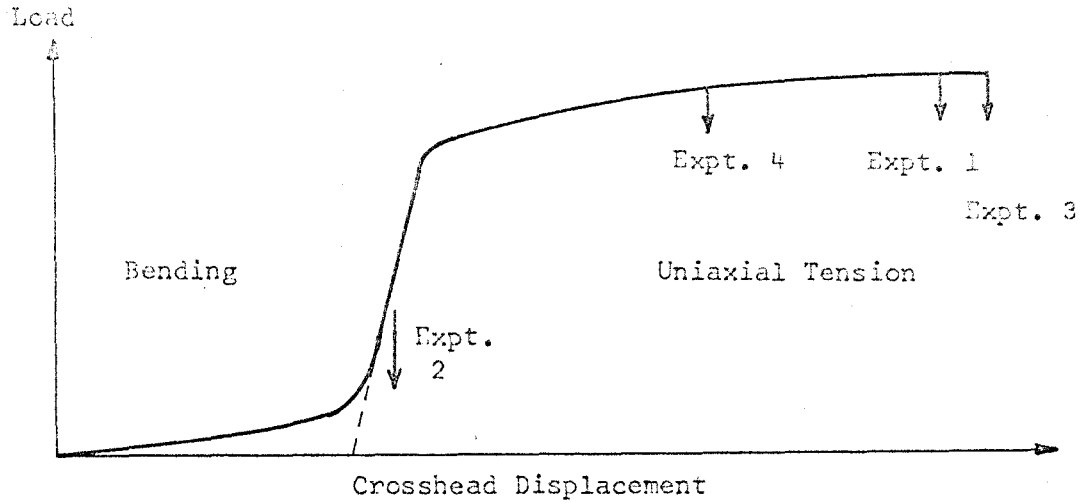

Fig. 9 SCHEMATIC ILLUSTRATION OF THE COMBINED BEND-TENSILE EXPERIMENTS

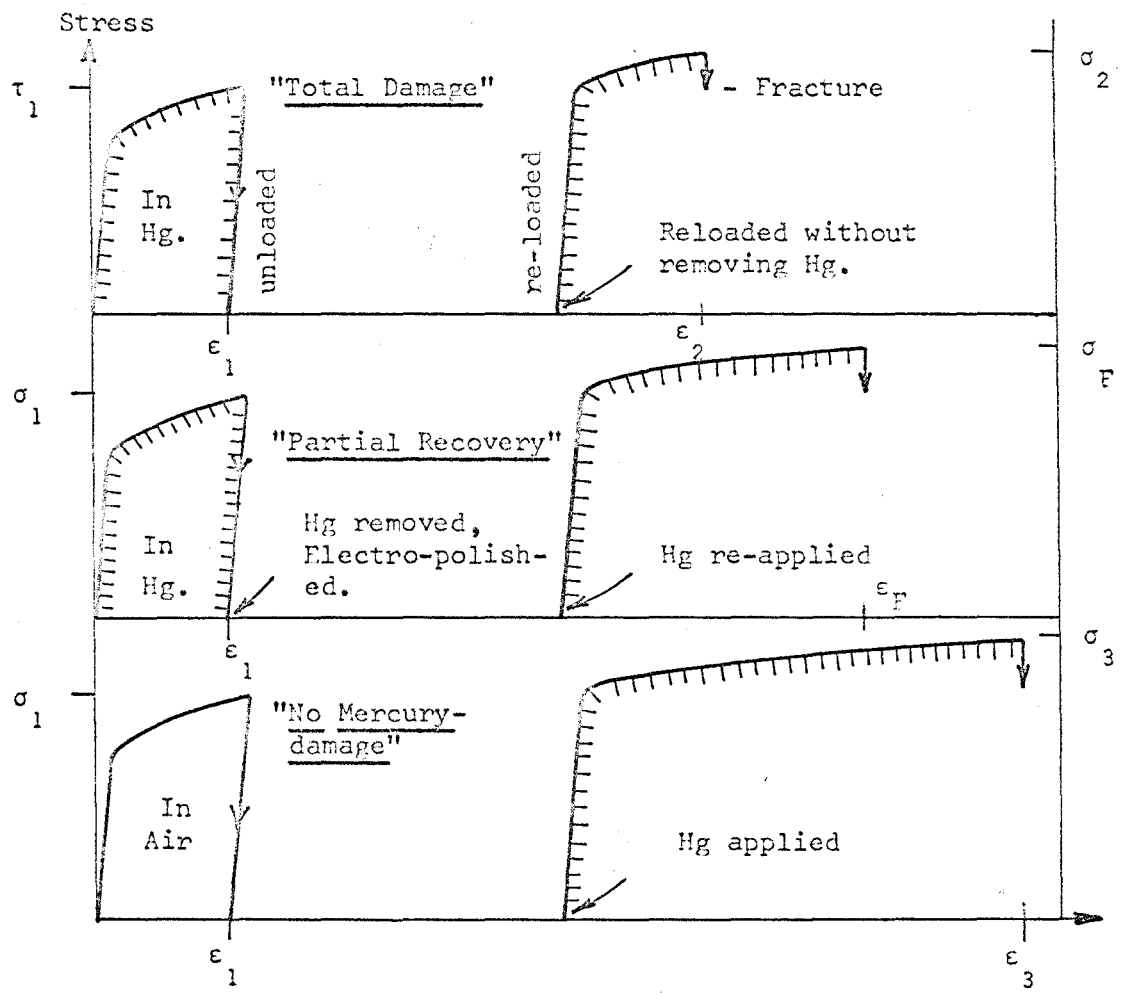

Fig. 10 SCHEMATIC ILLUSTRATION OF THE INTERMEDIATE ELECTRO-POLISHING EXPERIMENTS.

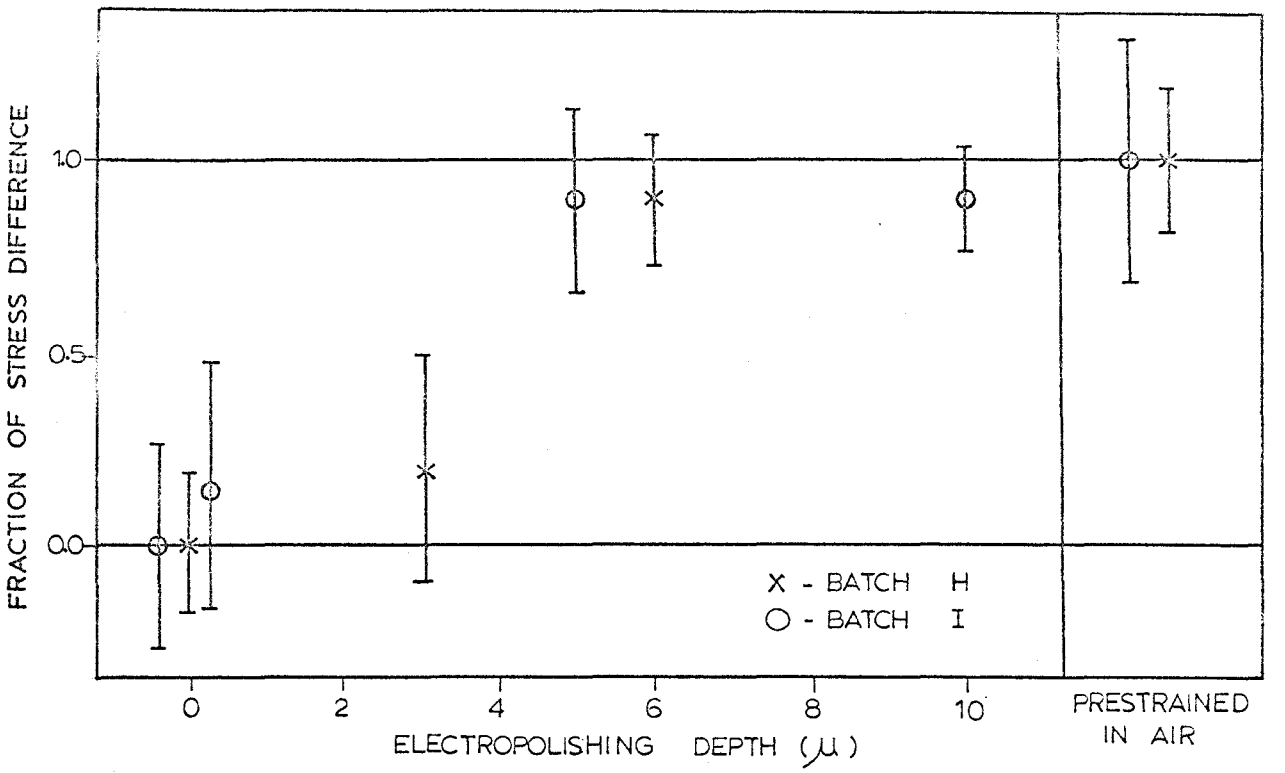

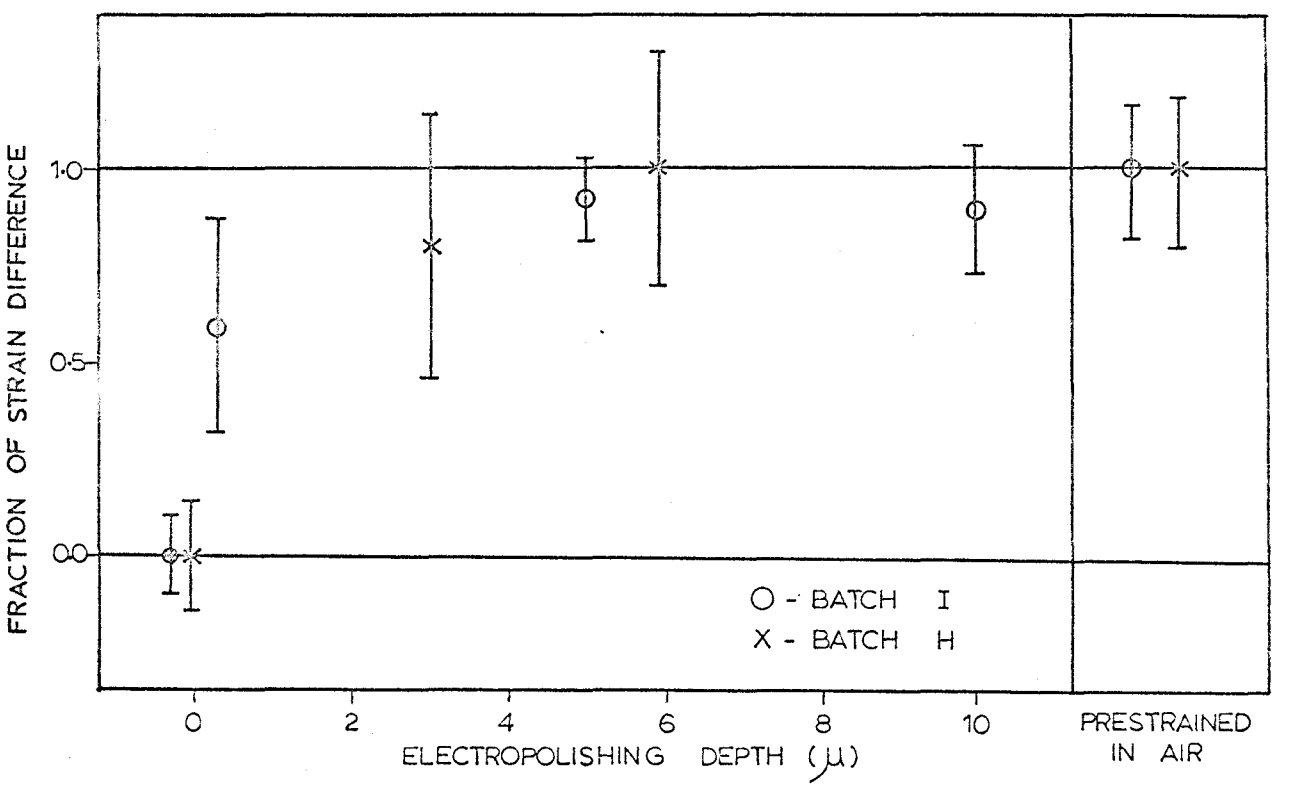

Fig. 11, ELECTROPOLISHING OF DAMAGED SURFACES

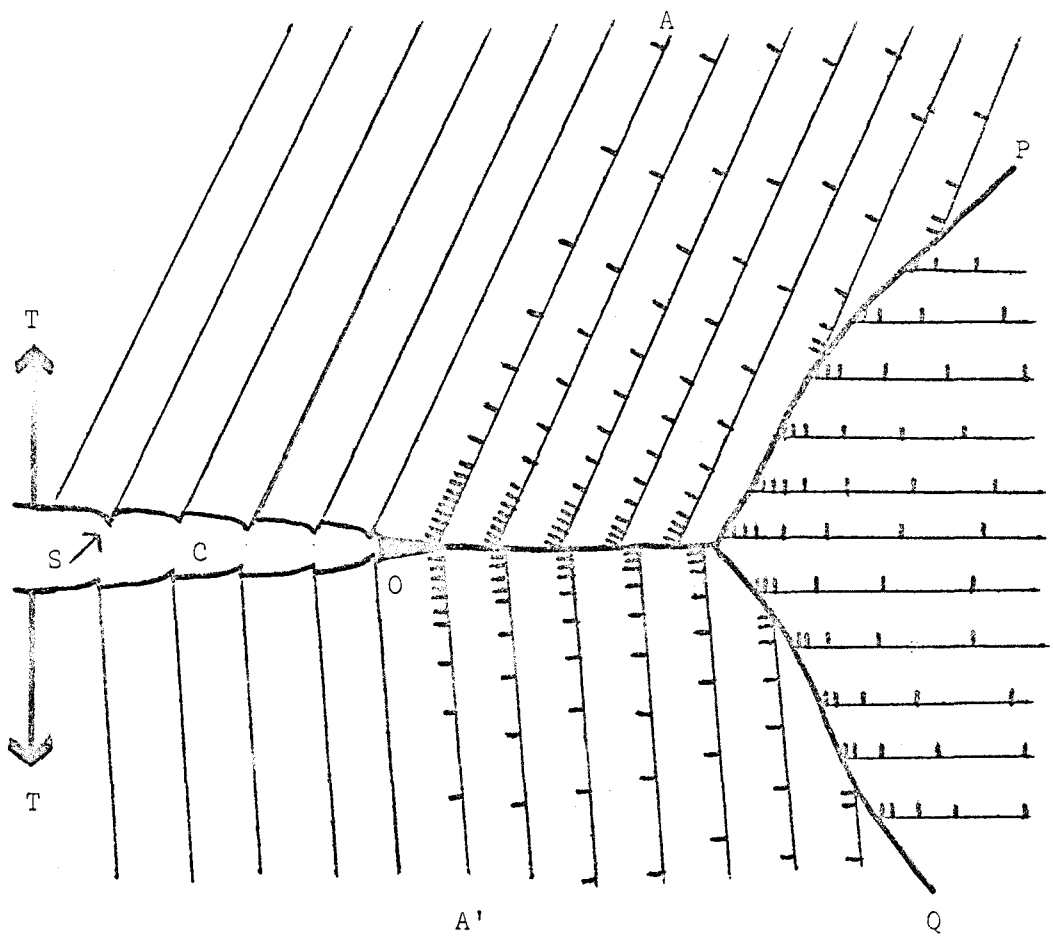

Fig. 12 SCHEMATIC MODEL OF DISLOCATION PILE-UP ARRAYS AROUND A MERCURY FILLED CRACK SUBJECTED TO A TENSILE FORCE T.

P-Q-O : Grain boundaries

C : Mercury filled crack

O : Micro-crack caused by pile-ups A, A' in a segment of grain boundary penetrated by mercury. The micro-crack causes an incremental extension of the crack C.

S : Slip steps on the fracture face, probably formed when pile-ups run into the crack.

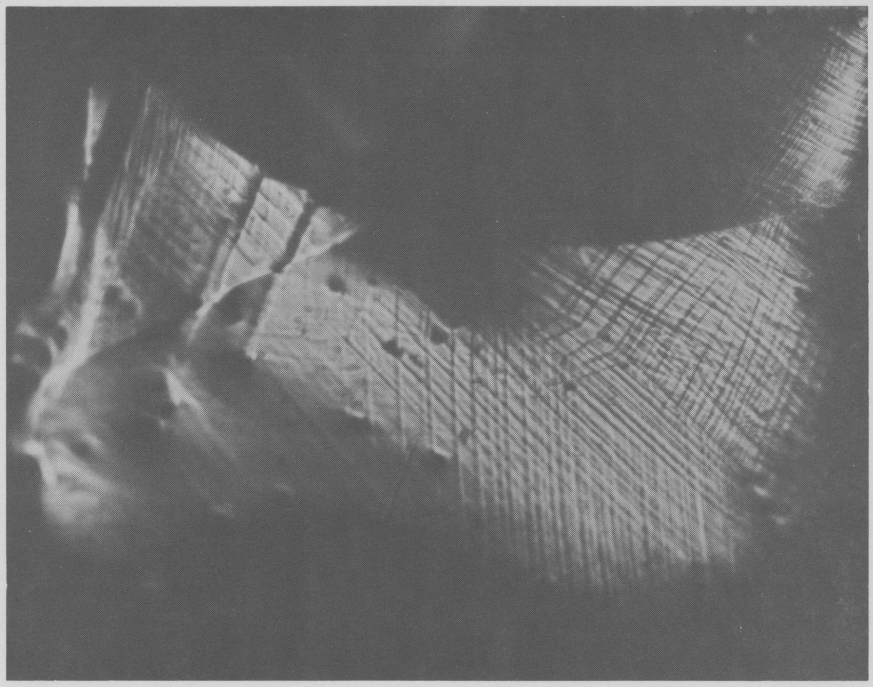

Plate A x150

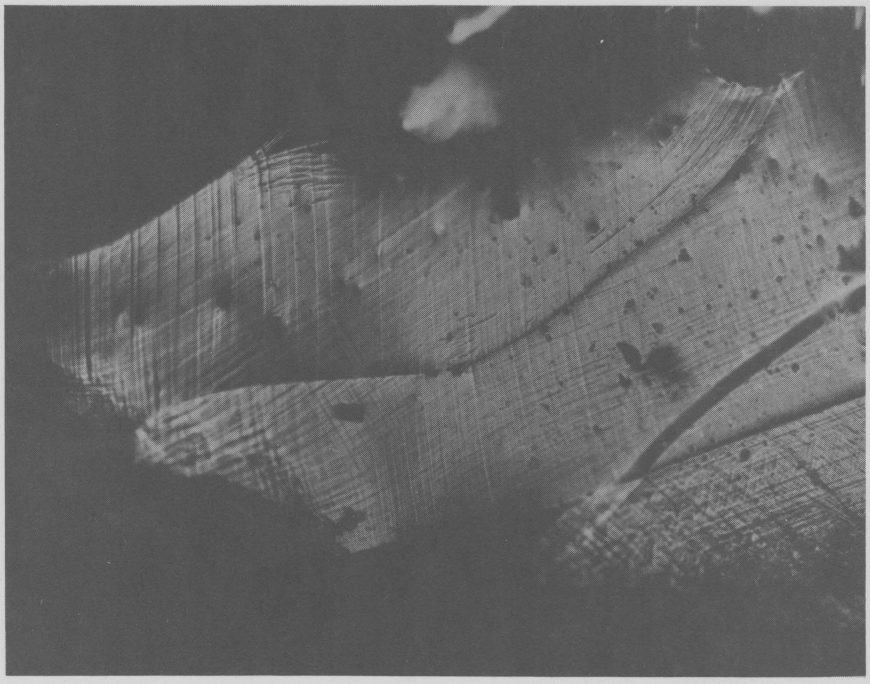

Plate B x150

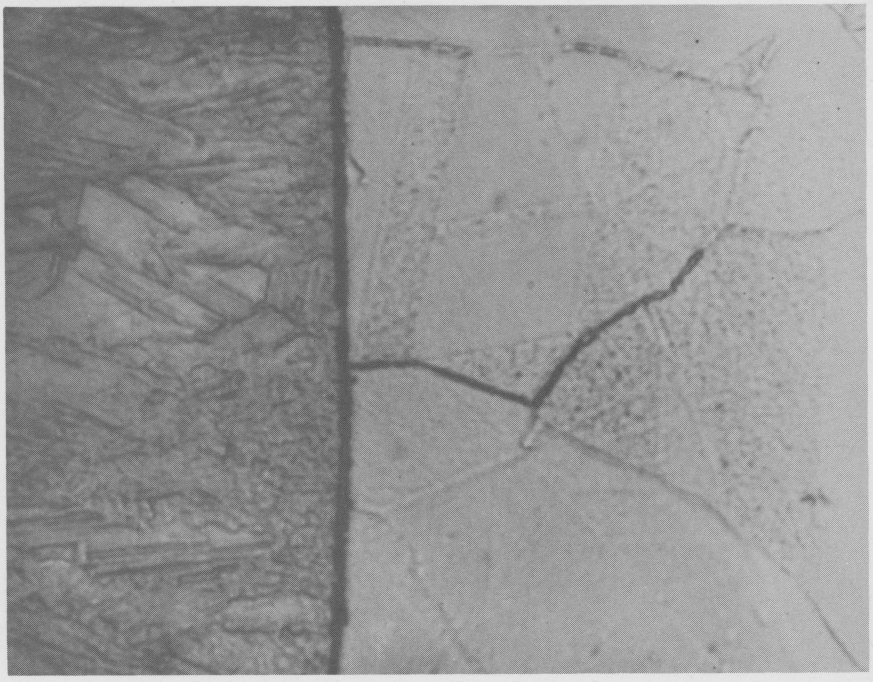

Plate C x1600

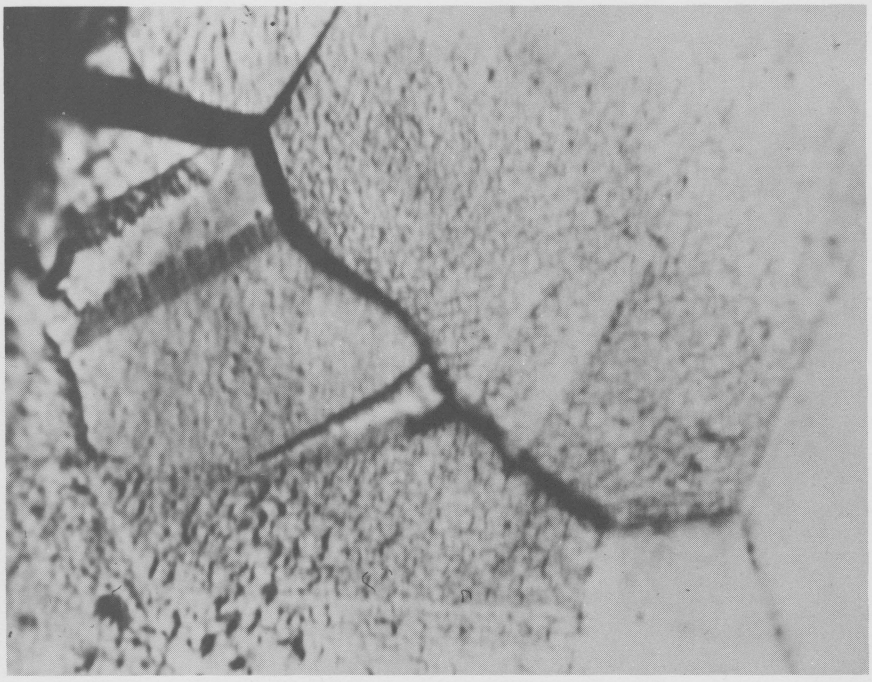

Plate D x2000

TABLE 1

X-RAY DIFFRACTION LIVE BROADENING DUE TO PLASTIC DEFORMATION

Specimen E_6		Specimen E_2	
Depth mm.	Line broadening mins. #	Depth mm.	Line broadening mins. #
0.003	8.9	0.013	7.8
0.007	7.1	0.053	5.0
0.100	4.7	0.093	4.5
0.22	4.2	0.220	4.2
0.320	2.8	0.280	4.2
0.960	2.1	0.430	3.5
		0.850	3.0
0.0 (E_{12})	6.5		

Table 1 X-ray diffraction line broadening due to plastic deformation as a function of depth below the fracture surface.

The line width of an annealed specimen has been subtracted from the measured widths to give the broadening due to plastic strain.

Measured uniform true strains at fracture are:

E_6: $\varepsilon_F = .058$

E_2: $\varepsilon_F = .048$

E_{12}: $\varepsilon_F = .050$

TABLE 2

MICRO-HARDNESS TESTS

Specimen E_7		Specimen Z_{11}	
Depth mm.	D.P.H. No.	Depth mm.	D.P.H. No.
0.024	150.5 ± 2.8	0.025	146.5 ± 1.7
0.050	144.0 ± 1.4	0.50	127.5 ± 1.5
0.105	141.7 ± 1.9		
0.200	135.2 ± 2.2		
0.300	130.3 ± 1.1		
0.750	128.2 ± 1.9		

Table 2 Micro-hardness tests on fracture specimens showing the variation of D.P.H. number with depth below the fracture surface.

Each value is the mean of at least 25 readings and the errors quoted are standard errors for 95% confidence.

TABLE 3

PLASTIC DEFORMATION AT THE FRACTURE SURFACE

Specimen	Work of Plastic Deformation $ergs/cm^2$	Plastic Strain at fracture surface	Estimated Shear flow stress at $crack_2$ surface Kg/mm^2
E_6	13.7×10^8	0.25	37
E_2	17.5×10^8	0.23	35
E_{12}	-	0.19	30
E_7	6.5×10^8	0.18	29
Z_{11}	-	0.12	23

Table 3 A summary of results obtained from x-ray diffraction line broadening and micro-hardness measurements at the fracture surface.

The work of plastic deformation is obtained from figure 2 by taking the area under the appropriate curve and subtracting the area under the uniform fracture strain ordinate appropriate to that specimen.

The shear flow stress estimate is taken from figure 3 as half of the tensile stress at a strain rate of 1800 per minute, corresponding to the plastic strain estimated above. This stress is a very approximate estimate and should be treated with some caution.

TABLE 4

STRESS AND STRAIN AT FRACTURE IN THE

COMBINED BEND-TENSILE EXPERIMENTS

Bending Strain %	Test No.	Fracture Strain # %	Fracture Stress p.s.i.
2.7	1	5.2 ± 0.20	33,200 ± 200
2.7	3	4.8 ± 0.40	34,100 ± 200
2.7	4	3.5 ± 0.25	26,600 ± 400
4.8	1	4.3 ± 0.10	30,800 ± 200
4.8	3	4.8 ± 0.15	32,000 ± 100
4.8	4	- *	- *
8.0	1	6.2 ± 0.25	32,700 ± 600
8.0	3	6.3 ± 0.20	33,500 ± 400
8.0	4	2.4 ± 0.15	27,100 ± 500

In test N°2, at all bending strains the specimens failed when the load curve reached the linear region (figure 9).

The strains at fracture refer to the strain in uniaxial tension only and do not include the strains in bending.

* Test N°4, was not performed for this bend radius.

The values given represent the mean of 5 tests and the errors quoted are one half of the total range.

TABLE 5 A, BATCH H

ELECTROPOLISHING OF DAMAGED SURFACES

Electropolishing Treatment (Reduction in radius)	Stress at Fracture, σ_F p.s.i.	Fraction of Stress difference $\frac{(\sigma_F - \sigma_2)}{(\sigma_3 - \sigma_2)}$	Strain at Fracture, ε_F %	Fraction of Strain difference $\frac{(\varepsilon_F - \varepsilon_2)}{(\varepsilon_3 - \varepsilon_2)}$
None	26,200 ± 285	0.0 ± .19	2.4 ± 0.15%	0.0 ± .15
3μ removed	26,500 ± 600	0.20 ± .30	3.2 ± 0.35%	0.8 ± .35
6μ removed	27,600 ± 285	0.93 ± .19	3.4 ± 0.35%	1.0 ± .35
(Prestrain in Air)	27,700 ± 285	1.0 ± .19	3.4 ± 0.20%	1.0 ± .20

TABLE 5 B, BATCH I

Electropolishing Treatment (Reduction in radius)	Stress at Fracture, σ_F p.s.i.	Fraction of Stress Difference $\frac{(\sigma_F - \sigma_2)}{(\sigma_3 - \sigma_2)}$	Strain at Fracture, ε_F %	Fraction of Strain difference $\frac{(\varepsilon_F - \varepsilon_2)}{(\varepsilon_3 - \varepsilon_2)}$
None	27,000 ± 410	0.0 ± .27	2.65 ± 0.10%	0.0 ± .11
0.2μ removed	27,200 ± 500	0.13 ± .33	3.20 ± 0.25%	0.60 ± .28
5μ removed	28,350 ± 350	0.90 ± .23	3.50 ± 0.10%	0.93 ± .11
10μ removed	28,400 ± 210	0.93 ± .14	3.50 ± 0.15%	0.93 ± .17
(Prestrain in Air)	28,500 ± 500	1.0 ± .33	3.56 ± 0.15%	1.0 ± .17

σ_F, σ_2, σ_3, ε_F, ε_2, ε_3 may be identified by reference to figure 10.

Each figure quoted is the mean of 5 values and the errors represent half of the maximum range.

APPENDIX I

CONDITIONS OF STRESS AND STRAIN AT THE CRACK-TIP

Kelly, Tyson and Cottrell (1967) have analysed the stress conditions at the tip of a crack in a material under plane strain as in figure A1. The crack is straight edged with $\varepsilon_{zz}=0$. The opposite surfaces must be smoothly closing if the stress at the tip is to remain finite. Biaxial tension is predicted at the tip with the maximum normal stress perpendicular to the plane of the crack and maximum shear stress on planes at 45^{o} to the z axis. By analysis of the ratio of normal stress across the cleavage plane to the maximum resolved shear stress on an observed slip system, the authors have attempted to predict for a variety of materials, which of two processes will occur first at the crack-tip if a continuously increasing tensile stress is applied across the crack. The two critical processes are, cleavage at the theoretical cohesive stress leading to true brittle fracture, and shear by generation of dislocations in the perfect lattice at the theoretical shear stress.

The approach used by these authors has been applied to the case of a crack containing liquid mercury at room temperature in polycrystalline pure copper and a Cu-17Al solid solution alloy. The results of the calculations are presented in tables at the end of this section. Data for elastic constants were obtained for copper from Overton and Gaffney (1955) and constants for Cu-17Al was obtained by extrapolation of the results of Neighbours and Smith (1954) for Cu-4.81Al and Cu-9.98Al alloys. Lattice parameters were obtained from Obinata and Wasserman (1933).

Kelly et al. have used a calculation of the theoretical shear stress due to Mackenzie (1949), which gives the shear stress for a low stacking fault, face-centred cubic metal as:

$$\tau_{max} = 0.039\ G'$$

where G' is the appropriate shear modulus for the slip system considered.

There is great uncertainty in the value of the true surface energy of the Cu_{sol}/Hg_{liq} and $Cu\text{-}17Al_{sol}/Hg_{liq}$ interfaces. An indirect measurement has been made by Greenwood (1953) in which the dihedral angle at a grain boundary in copper exposed to liquid mercury was 120°. The surface energy for Cu_{sol}/Hg_{liq} would therefore be equal to the grain boundary energy. Measurements of grain boundary energy give values around 600 to 800 ergs/cm^2 at temperatures in the region of 800°C. Even without correction for temperature these values are very much higher than those obtained by Pargeter and Ives (1967) from an analysis of the variation with grain size of the fracture stress of polycrystalline copper and Cu-Al solid solutions. This assessment of surface energy requires the prior assumption of a crack initiation model (Petch, 1953; Stroh, 1957) and is less direct than the dihedral angle measurements mentioned above. The high values obtained in the latter however are based upon the observations of Greenwood alone and no other measurements on this system are recorded in the literature. Interfacial energies for copper and brass in various environments are listed in table A6. In view of the uncertainty, calculations of cohesive strength have been made for a range of values of surface energy between 50 and 500 ergs/cm^2. A value of 300 ergs/cm^2 seems to be the most probable estimate in view of the recorded values for Cu_{sol}/Bi_{liq}, Cu_{sol}/Pb_{liq} and those for α- brass using dihedral angle

measurements, (table A6a). Dihedral angle measurements are preferred to those derived from grain size effects on the fracture stress (table A6b), since the technique is more direct and requires fewer prior assumptions.

Fig.A1

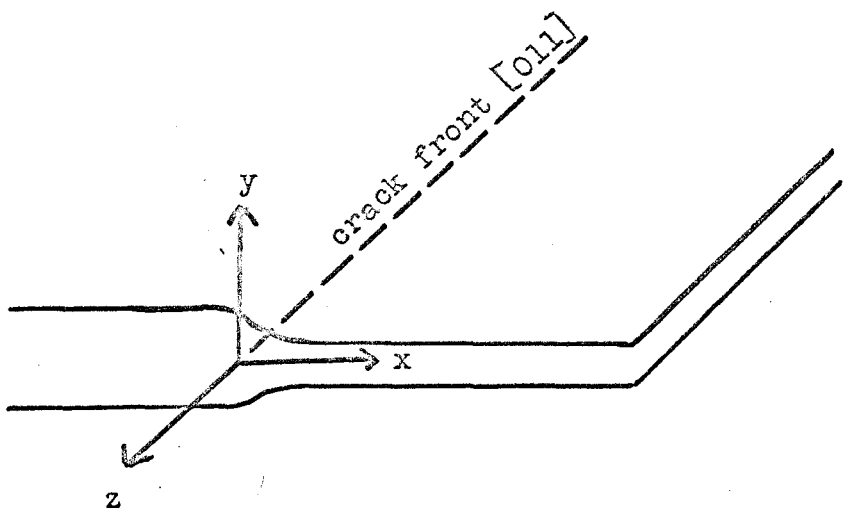

Fig. A1. The form of atomic planes bordering a smoothly closing crack on (111) with the crack edge along [011].

TABLE AI

VALUES OF COHESIVE STRENGTHS

	$\sigma_{max}\ 10^{10}$ dynes/cm^2		
	γ=50	γ=300	γ=500
Pure Cu.	4.28	10.50	
Cu-17Al.		9.42	12.20

Values of the theoretical cohesive strength, σ_{max}, across {100}, for various estimates of the true interface energy γ.

Values of γ are in ergs/cm^2.

Orowan's formula is:

$$\sigma_{max} = \left(\frac{E'\gamma}{a_o}\right) 1/2$$

E' is the appropriate Young's modulus: $E' = 1/S_{11}$, and values of E' are given in table A.5

a_o is the spacing of the {100} planes. Values of a_o are taken from Obinata and Wasserman (1933).

Pure Cu: a_o = 1.804 Å

Cu-17Al: a_o = 1.825 Å

TABLE A2

VALUES OF SHEAR FLOW STRESSES

	Shear Stress 10^{10} dynes/cm^2		
	τ_{max}	τ_1	τ_2
Pure Cu	1.19	0.127	0.107
Cu-17Al	1.03	0.093	0.006

τ_{max} is the theoretical shear stress given by Mackenzie's estimate (1949): $\tau_{max} = 0.039\ G'$.

G' is the shear modulus for slip on the $\{111\}\langle\bar{2}11\rangle$ or $\{111\}\langle 1\bar{1}0\rangle$ systems. Values are given in table A5.

τ_1 is the macroscopic shear flow stress taken as half the measured applied tensile stress at the point of fracture in polycrystalline material with a grain size of 0.04 mm.

τ_2 is a measure of the friction stress at the point of fracture, obtained from Pargeter and Ives (1967).

TABLE A3

RATIOS OF COHESIVE STRESS TO CRITICAL SHEAR STRESSES

	γ ergs/cm^2	$\frac{\sigma_{max}}{\tau_{max}}$	$\frac{\sigma_{max}}{\tau_1}$	$\frac{\sigma_{max}}{\tau_2}$
Pure Cu	50	3.61	33.8	40.1
"	300	8.83	82.7	98.1
"	500			
Cu-17Al	50			
"	300	9.10	101.5	157.7
"	500	11.83	127.5	203.5

Values of σ_{max} are taken from table A1; values of τ_{max}, τ_1 and τ_2 are taken from table A2.

The ratios given should be compared with the values of R in table A4.

TABLE A4

VALUES OF R.

	Stress System	R max	R min
Pure Cu	Plane Stress	3.7	2.0
	Plane Strain	11.5	6.3
Cu-17Al	Plane Stress	3.7	2.0
	Plane Strain	15.4	8.4

R is given by the ratio of maximum normal stress, (σ_1) max, across cleavage plane to the maximum resolved shear stress, τ', on an observed slip system.

$$R = \frac{(\sigma_1)_{max}}{\tau'} = \frac{K}{(1-2\upsilon')} \quad \text{for plane strain,}$$

and $$R = \frac{(\sigma_1)_{max}}{\tau'} = K \quad \text{for plane stress.}$$

Variations in the crack orientation with respect to the slip system give rise to extreme values of 2.0 and 3.7 for the factor K.

Poisson's ratio υ', has been taken as 0.34 for all crack orientations in copper, and as 0.38 for Cu-17Al.

TABLE A5

ELASTIC CONSTANTS FOR COPPER AND COPPER-ALUMINUM ALLOYS.

	Elastic constants and moduli						
	C_{11}	C_{12}	C_{44}	S_{11}	E'	G'	υ'
Cu	16.87	12.16	7.57	1499	6.71	3.06	0.418
Cu-4.81Al	16.58	12.16	7.49	1590	6.29	2.89	0.423
Cu-9.98Al	15.95	11.76	7.66	1675	5.97	2.77	0.425
Cu-17Al	-	-	-	-	5.53	2.61	0.429

All units are 10^{11} dynes/cm^2.

E' is Young's modulus appropriate to ⟨100⟩

$$E' = {}^{1}/_{S_{11}}$$

υ' the appropriate Poisson's ratio:

$$\upsilon' = {}^{S_{12}}/_{S_{11}} = {}^{C_{12}}/_{(C_{11} + C_{12})}$$

G' is the shear modulus for slip on the system {111}⟨$\bar{2}$11⟩

$$G' = \frac{3C_{44}\,(C_{11} - C_{12})}{4C_{44} + C_{11} - C_{12}}$$

Elastic stiffness constants have been taken for Cu from Overton and Gaffney (1955) and for the Cu-4.81Al and Cu-9.98Al from Neighbours and Smith (1954). Values of S_{11}, E', G' and υ' have been calculated for these metals and extrapolated to give values for Cu-17Al.

TABLE A6a.

INTERFACIAL ENERGIES.

Interface	γ ergs/cm^2	Temperature °C	Reference
Cu_S/Cu_L	1730	1000	Inman and Tipler (1963)
Cu_S/Pb_L	390	350	Morgan (1954)
Cu_S/Bi_L	280	350	Morgan (1954)
$Brass_S/Hg_L$	498	20	Waterhouse and Grubb (1962)
$Brass_S/Bi_L$	280	350	Rostoker (1960)
Cu (grain boundary)	613	1000	Inman and Tipler (1963)
Cu (stacking fault)	71	20	Venables (1954)

S solid, V vapour, L liquid.

Table A6a: Interfacial energies for Copper and Copper Alloys measured by thermal etching or dihedral angle techniques.

Inman and Tipler (1963) give the temperature coefficient of the surface energies for metals as lying between -0.5 and -2.5 ergs/cm^2/°K. McLean (1957) quotes a coefficient of -0.5 for solid surface free energy and estimates -0.7 ergs/cm^2/°K for interfacial free energies.

TABLE A6b.

INTERFACIAL ENERGIES.

Interface	γ ergs/cm^2	Temperature C	Reference
Cu_S/Bi_L	160 or 91 ≠	350	Rostoker (1960)
Cu_S/Li_L	1010	200	Rostoker (1960)
Cu_S/Hg_L	48	20	Pargeter and Ives (1967)
$Cu\text{-}4.3Al_S/Hg_L$	70	20	Pargeter and Ives (1967)
$Cu\text{-}8.5Al_S/Hg_L$	175	20	Pargeter and Ives (1967)
$Cu\text{-}13Al_S/Hg_L$	377	20	Pargeter and Ives (1967)
$Cu\text{-}17Al_S/Hg_L$	471	20	Pargeter and Ives (1967)
$\alpha Brass_S/Bi_L$	920 ≠ or 525	350	Rostoker (1960)
$\alpha Brass_S/Hg_L$	270	20	Rostoker (1960)

≠ Two different analyses of the same data.

Table A6b: Interfacial energies measured from variation of fracture stress with grain size.

REFERENCES

1. Barclay W. and Rhines F. N. (Unpublished Carnegie Institute of Technology).

2. Bryukhanova L. S., Andreeva I. A. and Likhtman V.I. (1962) Soviet Physics (Solid State) 3, 2025.

3. Felbeck O.K. and Orowan E. (1955), Welding J. (Res. Supp.) 34, 570-s.

4. Gilman J. J. (1958), Trans. Met. Soc. A.I.M.E. 212, 783.

5. Gilman J. J. (1959), Fracture, Swampscott Conference , 193

6. Greenwood J. N. (1953), J. Inst. Met. 81, 177.

7. Griffith A. A. (1921), Phil. Trans. Roy. Soc. (Lond.) A221, 163.

8. Inman M.C. and Tipler H. R. (1963), Metall. Rev. 8, 105.

9. Johnston R. L., Davies R. G. and Stoloff N. S. (1965) Phil. Mag. 12, 305.

10. Kelly A. (1966), Strong Solids, Clarendon Press, Oxford.

11. Kelly A., Tyson W. R. and Cottrell A. H. (1967) Phil. Mag. 15, 567

12. Levine E. and Cadoff I. (1964), Trans, Met. Soc. A.I.M.E. 230, 1116.

13. Likhtman V. I. Shchukin E. D. and Rebinder P. (1962), Physico-Chemical Mechanics of Metals, Akad. Nauk. U.S.S.R. 163.

14. Mackenzie J. K. (1949), Ph.D. Thesis. Bristol University.

15. McLean D. (1957), Grain Boundaries in Metals, (Clarendon Press, Oxford).

16. Morgan W. A. (1954), Ph.D. Thesis. Cambridge University.

17. Neighbours J. R. and Smith C. S. (1954), Acta Met. 2, 591.

18. Nichols H. and Rostoker W. (1965), Trans. A.S.M. 58, (2), 155.

19. Obinata I. and Wasserman G. (1933), Naturwiss 21, 382. (From "Handbook of Lattice Spacings in Metals and Alloys," Pearson).

20. Orowan E. (1949), Rep. Prog. Phys. 12, 185.

21. Oho H. (Unpublished) Denver Research Institute.

22. Overton W. C. and Gaffney J. (1955), Phys. Rev. 98, 969.

23. Pargeter F. W. J. and Ives M. B. (1967) Can. J. Phys. 45, 1235.

24. Petch N. J. (1953), J. Iron Steel Inst. 174, 25.

25. Rinnovatore J. V., Corrie J. D. and Markus H. (1966) Trans. A.S.M. 59, (4), 665.

26. Rogus B. J. (1966), Trans. A.S.M. 59, (2), 240.

27. Rosenberg R. and Cadoff I. (1963), Fracture in Solids, (Interscience, New York) 607.

28. Rostoker W., McCaughey J. M. and Markus H. (1960), Embrittlement by Liquid Metals, (Reinhold, New York).

29. Shchukin E. D., Kochanova L. A. and Pertsov N. V. (1963) Soviet Physics (Crystallography), 8, 49.

30. Smith C. S. (1953) Trans. A.S.M. 45, 533.

31. Stroh A. N. (1957), Adv. in Phys. 6, 418.

32. Tabor D. (1951), The Hardness of Metals, (Clarendon Press, Oxford).

33. Verables J. (1964), J. Phys. Chem. Solids. 25, 685.

34. Waterhouse R. B. and Grubb D. (1962), J. Inst. Met. 91, 216.

35. Westwood A. R. C. and Kamdar M. H. (1962), R.I.A.S. Report 62-19.

36. Westwood A. R. C. and Kamdar M. H. (1965), R.I.A.S. Report 65-3.